

Ultrafast Laser 3D Micro and Nanoprocessing

Koji Sugioka

Advanced Laser Processing Research Team

RIKEN Center for Advanced Photonics

Wako, Saitama 351-0198, Japan

E-Mail: ksugioka@riken.jp

Self-introduction



Koji Sugioka

Birthday: Oct. 26, 1961

Gender: Male

Title: Dr. Eng.

Doctor Honoris Causa (the University of Szeged, Hungary)

Fellow SPIE, OPTICA (formerly OSA), LIA, IAPLE, JSAP

Position: Team Leader

Institution: RIKEN

Department: RIKEN Center for Advanced Photonics

Laboratory Advanced Laser Processing Research Team

Address: 2-1 Hirosawa, Wako, Saitama 351-0198, Japan

E-Mail Address: ksugioka@riken.jp

Area of expertise: Laser micro and nano processing
from the fundamental aspects to applications



About RIKEN

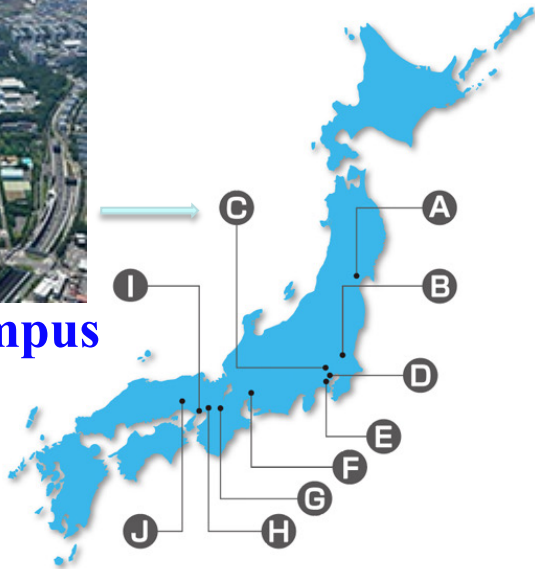
理研：理化学研究所(RIKAGAKU-KENKYUSHO)

RIKEN is the oldest institute for scientific research in Japan, founded in 1917.

RIKEN is then Japan's largest comprehensive research institution renowned for high-quality research in a diverse range of scientific disciplines including physics, chemistry, biology, neuroscience, computer science, engineering, etc.



Wako main campus



- A: Sendai Campus (Miyagi)
- B: Tsukuba Branch (Ibaraki)
- C: Wako Branch / Headquarters (Saitama)
- D: Tokyo Campus (Chuo-ku, Tokyo)
- E: Yokohama Branch (Kanagawa)
- F: Nagoya Branch (Aichi)
- G: Keihanna Campus (Keihanna Science City, Kyoto)
- H: Osaka Campus (Osaka)
- I: Kobe Branch (Hyogo)
- J: Harima Branch (Hyogo)

Overseas Offices

- A: RIKEN Facility Office at RAL (UK)
- B: Europe Office (Brussels, Belgium)
- C: Singapore Office (Singapore)
- D: Beijing Office (China)
- E: RIKEN BNL Research Center (New York, USA)

Outline

1. Fundamentals

- ◆ Principles of ultrafast laser 3D processing

2. Schemes of 3D Processing and Examples of Each Scheme

- ◆ Undeformative processing (Zero processing)
- ◆ Subtractive processing
- ◆ Additive processing

3. Hybrid 3D Processing

- ◆ Subtractive + undeformative processing
- ◆ Subtractive + additive processing
- ◆ Additive + subtractive processing

4. Summary

1. Fundamentals

Characteristics of ultrafast laser processing

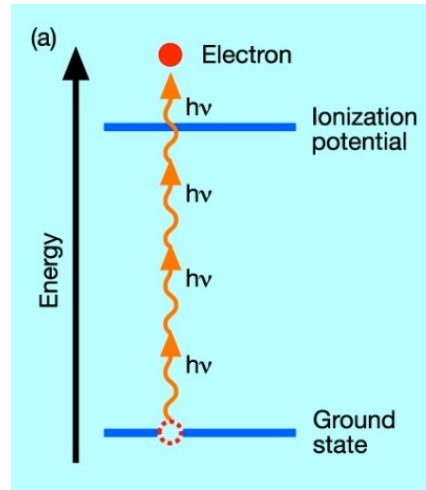
Wavelength: 800 nm ~ 1 μm (typically 1 μm)
Visible and UV are available by use of harmonics

Pulse width: Several tens of fs ~ tens of ps
(several tens ~ several hundred of fs for research,
several ps for industrial applications)

Peak intensity: ~ several tens of PW/cm² (10¹⁵/cm²)

- ◆ **Minimized heat affected zone.**
- ◆ **Processing of transparent materials by multiphoton or tunneling ionization.**
- ◆ **Internal modification & 3D fabrication of transparent materials.**
- ◆ **Nanofabrication with a resolution beyond diffraction limit.**

Nonlinear absorption process of ultrafast laser by transparent materials

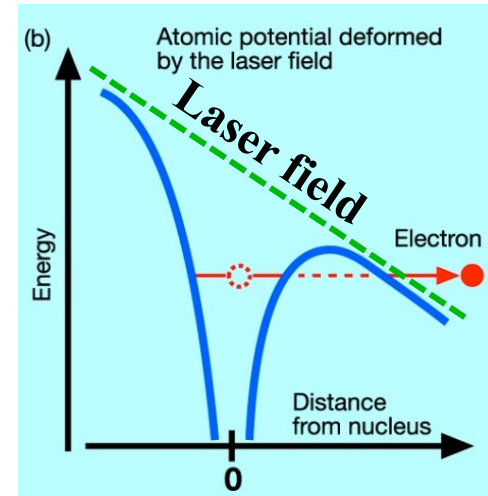


Multiphoton absorption
($\gamma \gg 1$)

Keldysh parameter

$$\gamma = \frac{\omega}{e} \sqrt{\frac{m_e c n \epsilon_0 E_g}{I}}$$

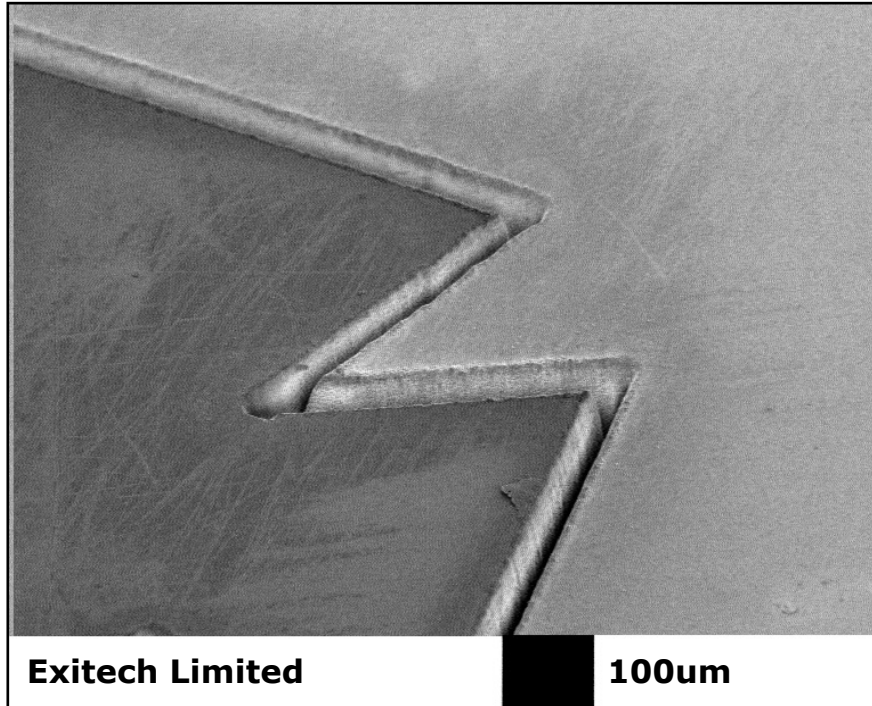
Waveguide writing: typical $\gamma = \sim 1$



Tunneling ionization
($\gamma \ll 1$)

ω : laser frequency, I : laser intensity, m_e : electron effective mass, e : fundamental electron charge, c : speed of light, n : linear refractive index, ϵ_0 : permittivity of free space, E_g : band gap

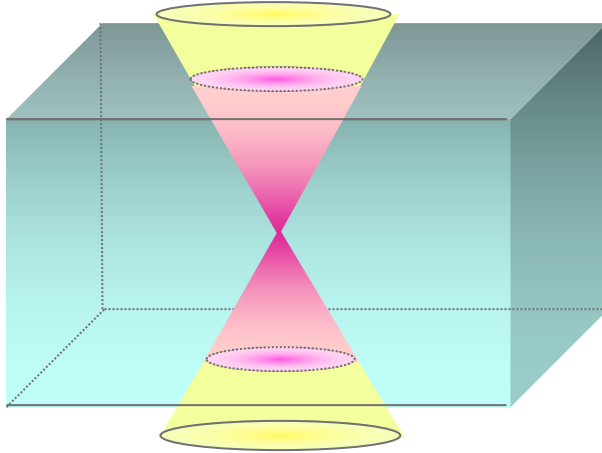
Ablation of transparent material



Wavelength : 800 nm
Material: Fused silica

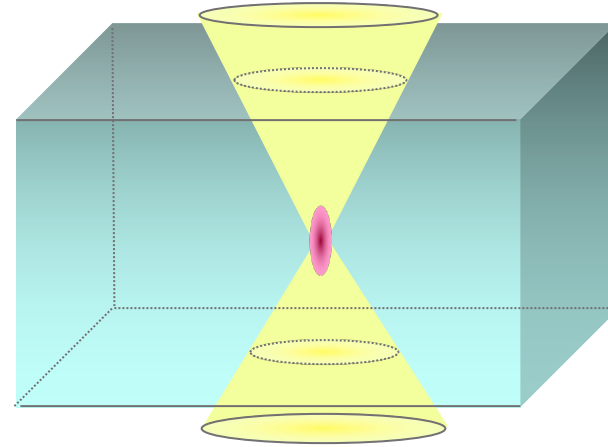
By courtesy of M Gower.

Internal modification and 3D processing of transparent materials



Single-photon

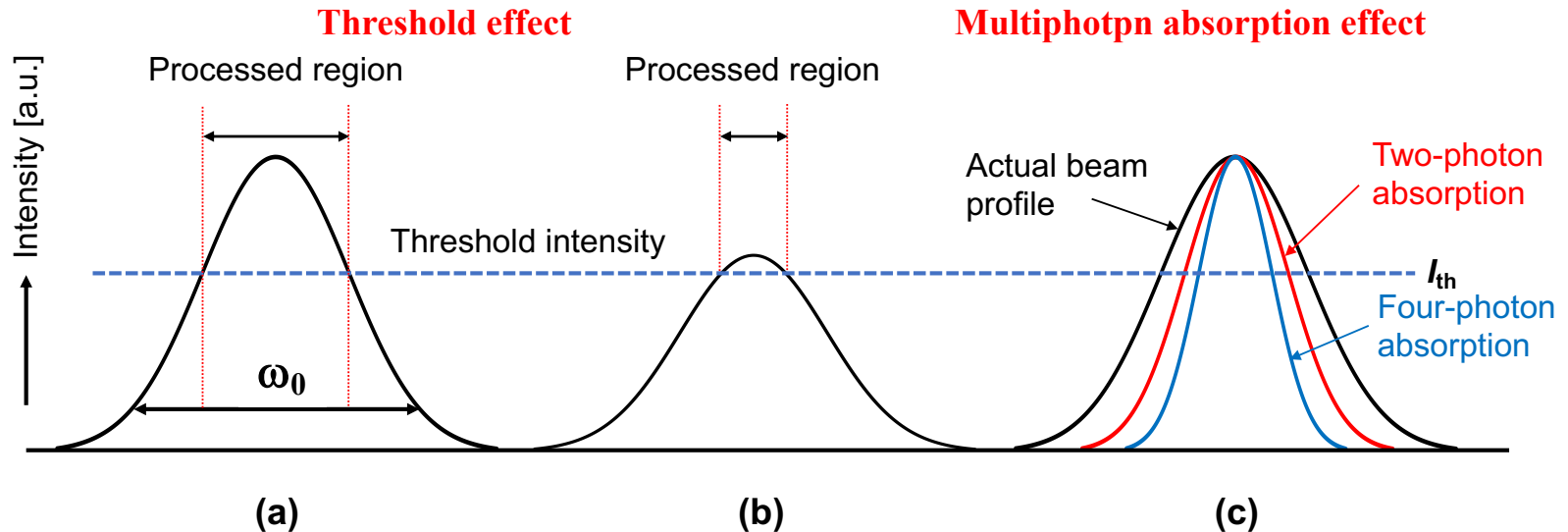
- *Photoreaction occurs from the surface of material*
- *Poor axial resolution*
- *Limited penetration depth*



Multi-photon

- *Photoreaction occurs only near the focus*
- *Improved axial resolution*
- *Enhanced penetration depth*

Fabrication resolution far beyond diffraction limit



(a) The closer the laser intensity at the center of the focused laser beam is to the threshold value, the narrower the processed area.

$$\omega_0 = 1.22\lambda/NA: \text{diffraction limit}$$

Typical fabrication resolution of TPP: ~ 100 nm

(NA = 1.4, λ = 800 nm, Spot size: ~ 700 nm)

Effective beam diameter for n-photon absorption ω ;

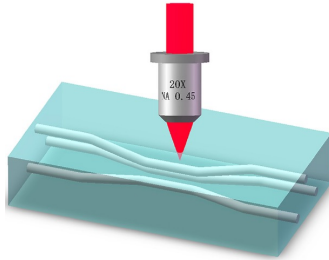
$$\omega = \omega_0 / \sqrt{n} \quad (\omega_0 : \text{Actual beam diameter})$$

(Probability of n-photon absorption depends on I^n)

2. Schemes of 3D Processing and Example of Each Scheme

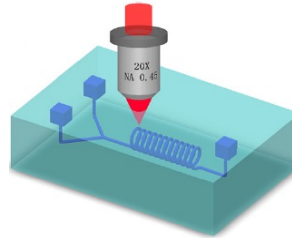
Ultrafast Laser 3D Processing

Undeformative processing (Zero processing)

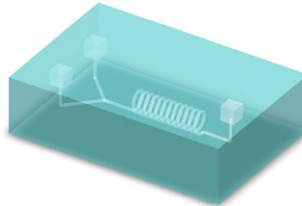


**Internal refractive index
modification inside glass**

Subtractive processing



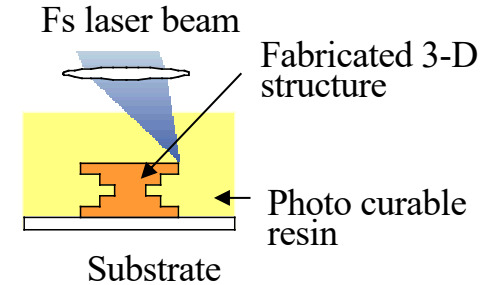
(1) Ff laser direct writing



(2) HF etching

**Femtosecond laser 3D
glass micromachining**

Additive processing

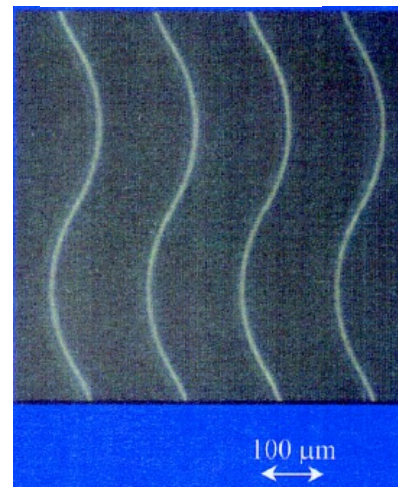
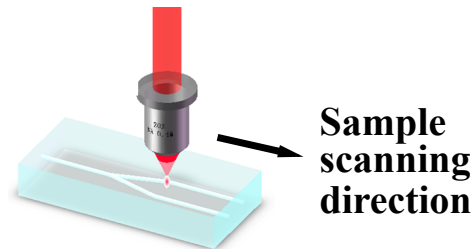
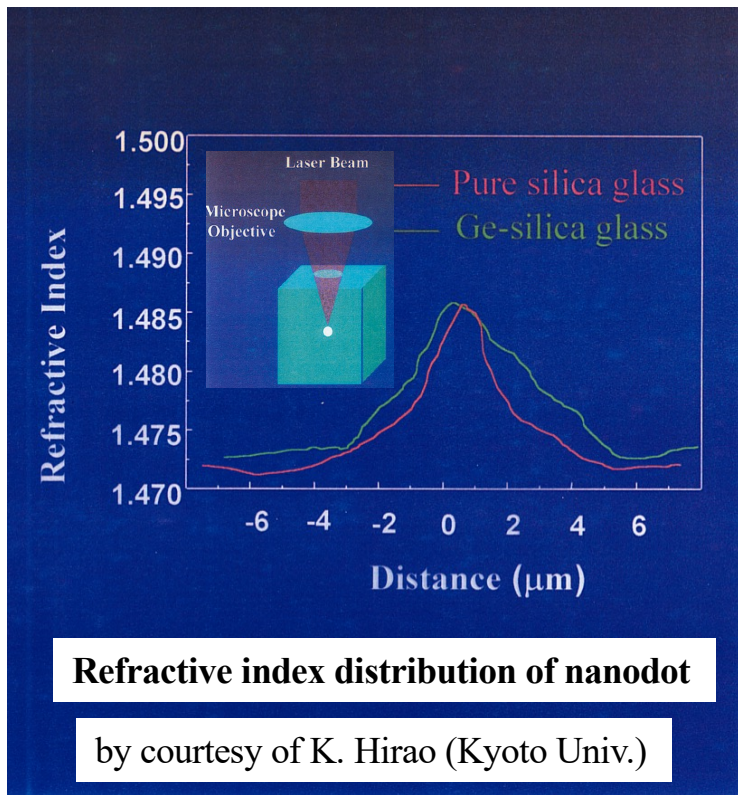


**Two-photon polymerization
(TPP)**

Undeformative Processing

Internal Refractive Index Modification of Glass (**waveguide writing**)

K. M. Davis et al., Opt. Lett. **21**, 1729 (1996).

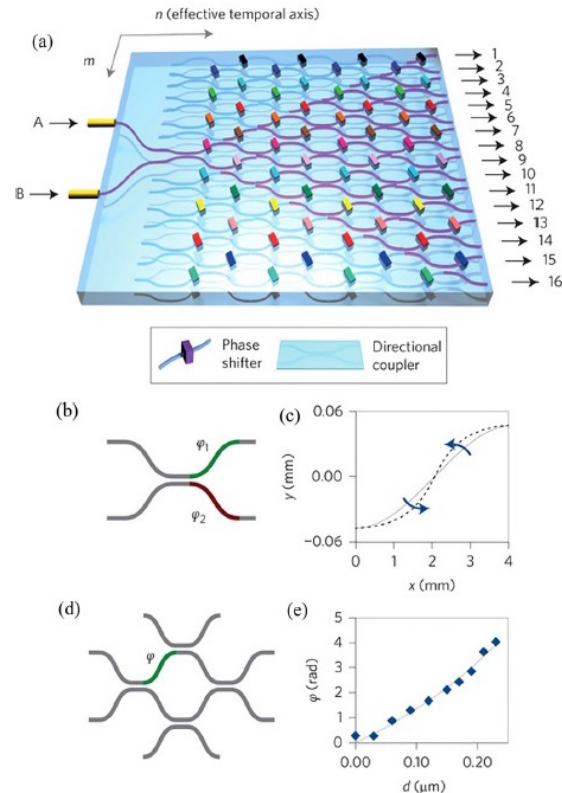


Optical waveguide embedded in fused silica

Undeformative Processing: Internal Refractive Index Modification

3D Photonic Devices

- ◆ Optical waveguide
- ◆ Optical coupler and splitter
- ◆ Mach-Zehnder interferometer
- ◆ Diffraction grating
- ◆ Diffractive lens
- ◆ Bragg grating
- ◆ Waveguide laser
- ◆ Compact quantum circuit
*for quantum computing
and quantum network*



Compact Quantum Circuit Chips
consisting of an interferometric array to
simulate an eight-step 1D quantum walk

Internal Refractive Index Modification of Transparent Materials

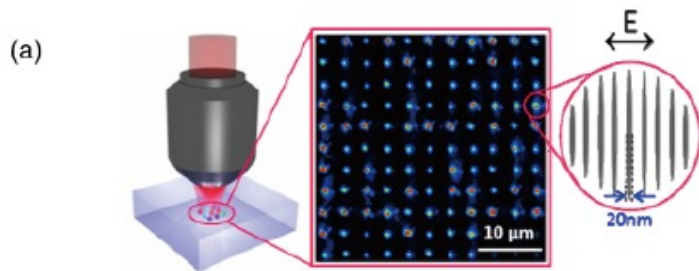
Materials

- **Glass:** fused silica, borosilicate glass, chalcogenide glass, Foturan glass, etc.
- **Crystal:** Ti:Sapphire, Nd:YAG, Yb:YAG, Nd: YLF (LiYF_4), LiNbO_3 , etc.
- **Semiconductor:** Si, Diamond, GaAs, etc.
- **Polymer:** PMMA, CYTOP, etc.

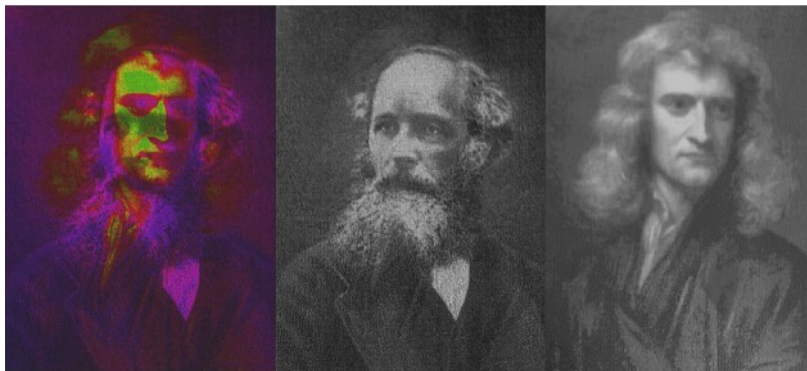
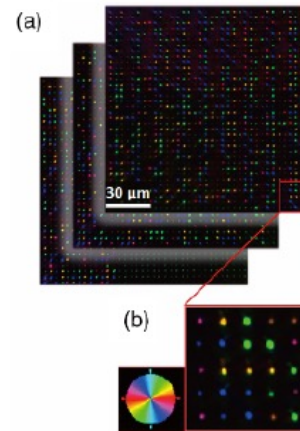
*Wavelength of ultrafast laser must be transparent.
e.g., $1.5 \mu\text{m}$ for Si*

Applications of Internal Refractive Index Modification

5D Data Storage



Formation of dot structures in which nanograting is formed to induce birefringence where the axial orientation and strength of retardance are used as the fourth and fifth dimensions



Maxwell

Newton

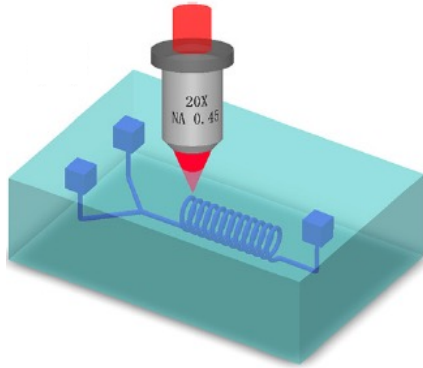
Left: Mixed image (in pseudo color)
Center: Recorded in strength of retardance
Right: Recorded in azimuth of the slow axis

Subtractive Processing

Ultrafast Laser Assisted Etching (**ULAE**)

Ultrafast Laser Induced Selective Etching (**ULISE**)

Ultrafast laser direct write



Formation of 3D modified regions

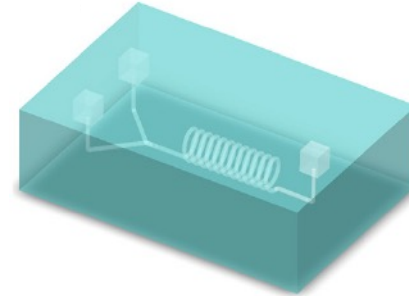
Materials

- Fused silica (wide transparency, high purity)
- Photosensitive Foturan glass (smooth surface, selective metallization)

Chemical etching

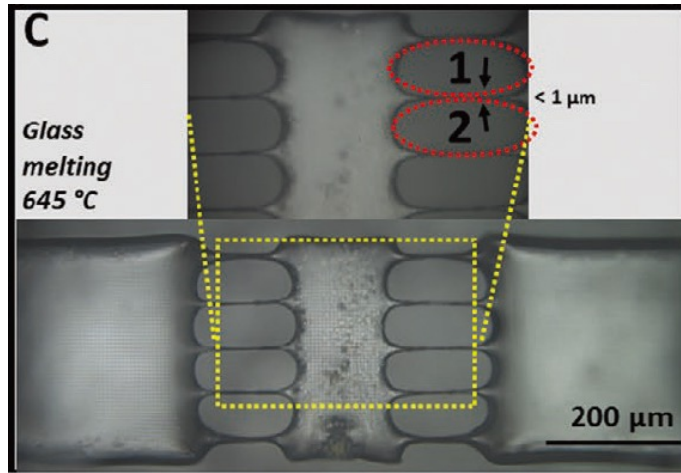
in diluted HF

Contrast ration in etching selectivity: 30 ~ 50

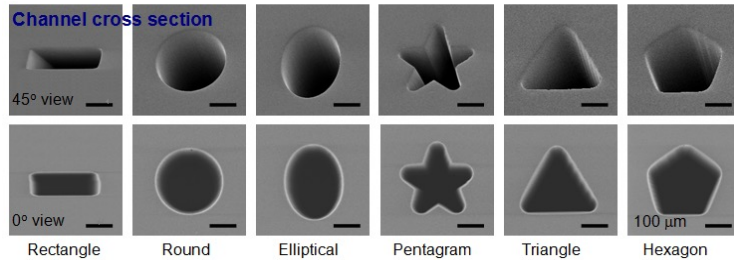


Formation of 3D hollow microstructures

Fabrication of 3D Glass Micro/Nanofluidic Chips



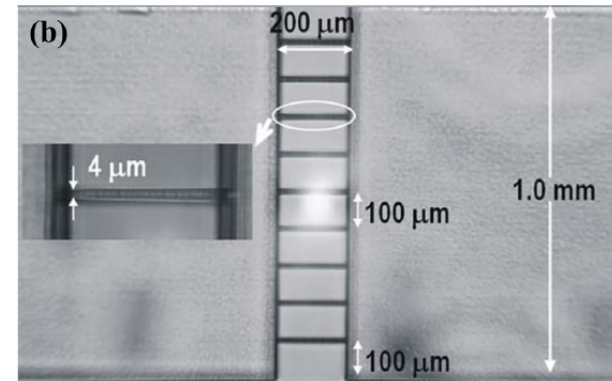
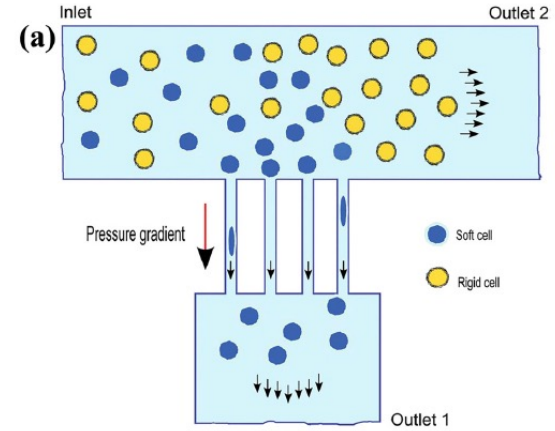
3D nanofluidics



Controllable cross-sectional shape of microchannel

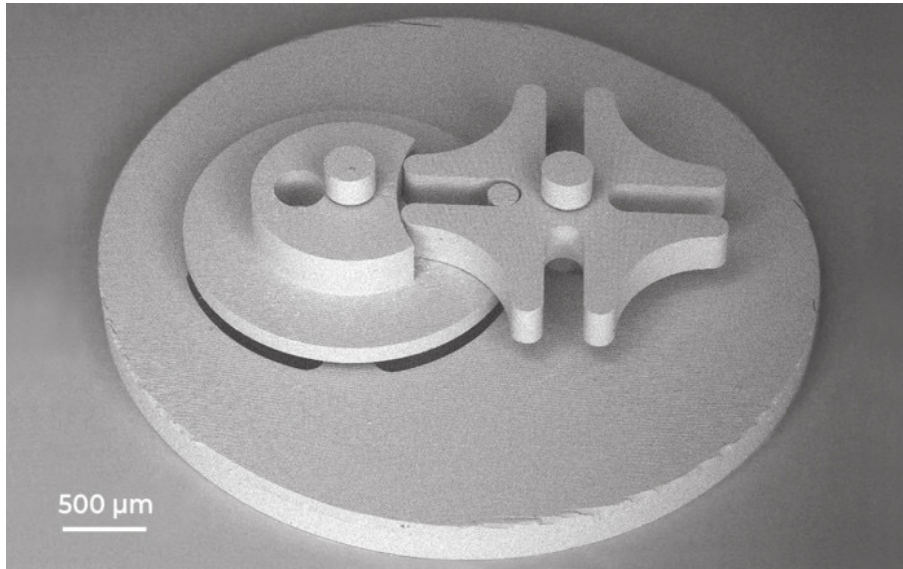
K. Sugioka et al., *Laser Photon Rev.* **4**, 386 (2010).

F. Sima, Ksugioka et al., *Adv. Mater. Technol.* **5**, 2000484 (2020).



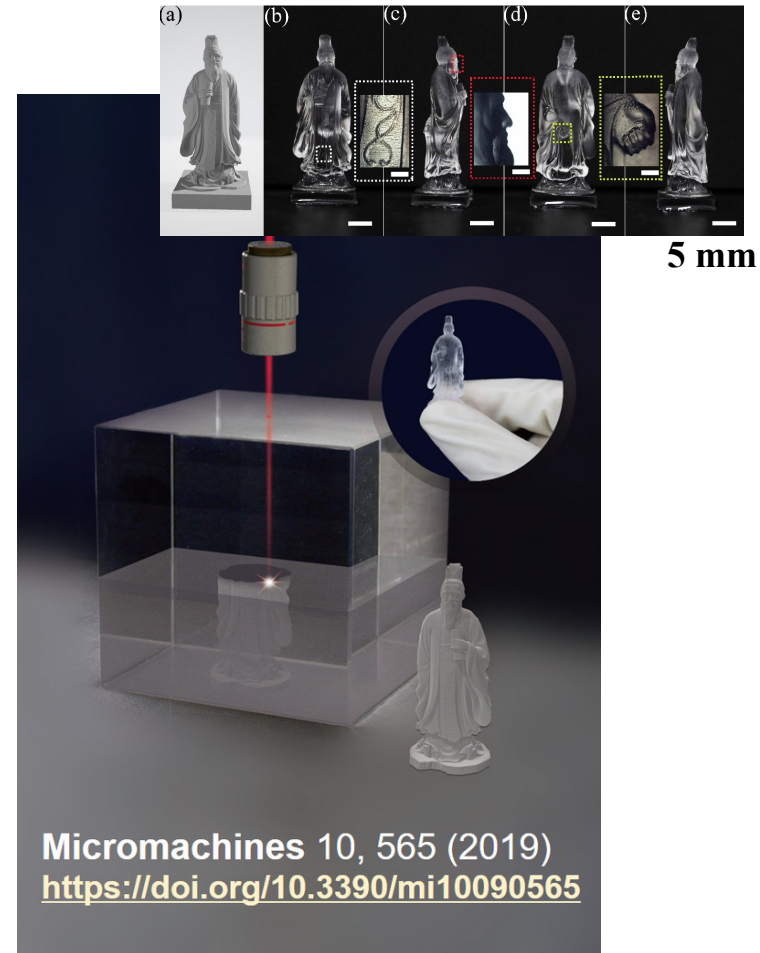
Choudhury et al., *Lab Chip* **12**, 948 (2012).

Fabrication of mm to cm Scale 3D Objects



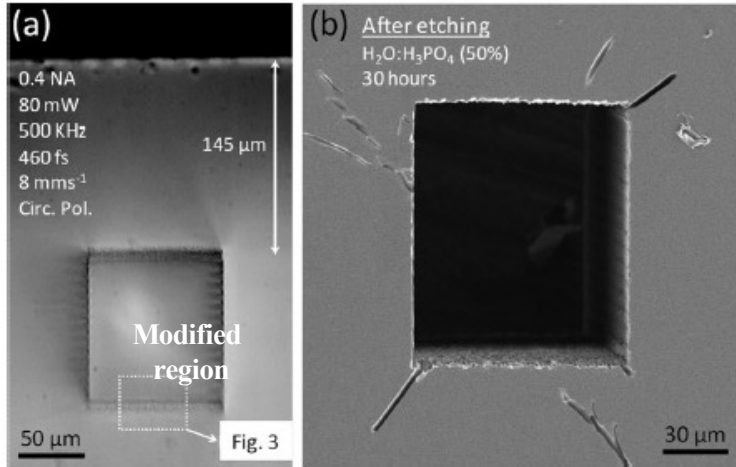
Geneva Gear

<https://femtika.com/example/geneva-gear/>



Micromachines 10, 565 (2019)
<https://doi.org/10.3390/mi10090565>

Materials Available for ULAE

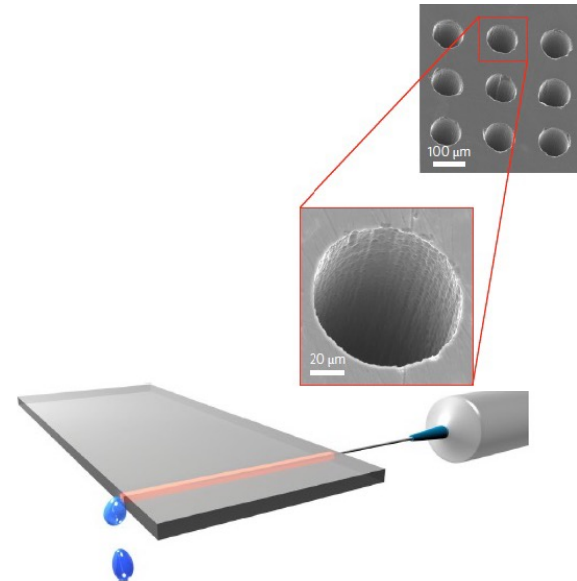


Nd: YAG

Laser wavelength: 1047 nm

Etchant: Orthophosphoric acid (H₃PO₄)

D. Choudhury et al., Appl. Phys. Lett. **103**, 041101 (2013).



Si

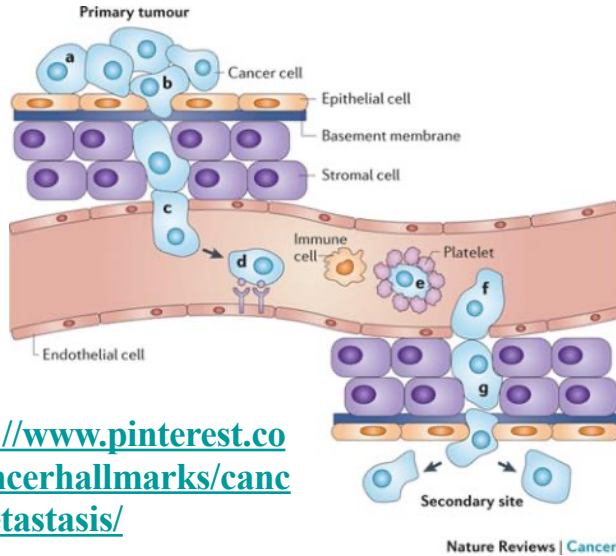
Laser wavelength: 1.55 μm

Etchant: Cu(NO₃)₂, HF, HNO₃ and CH₃COOH

O. Tokel et al., Nature Photon. **11**, 639 (2017).

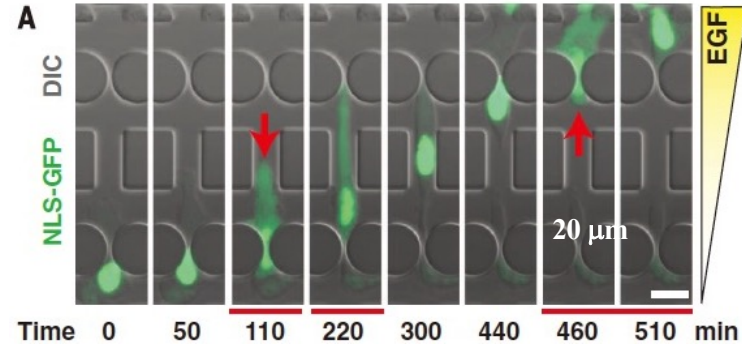
Application of 3D microfluidic chip

Mechanism study of cancer cell metastasis and invasion



<https://www.pinterest.com/cancerhallmarks/cancer-metastasis/>

At early stages of metastasis formation and cancer cell invasion in human body, cells must undergo large morphological changes in order to cross the basement membrane and move through connective tissue.



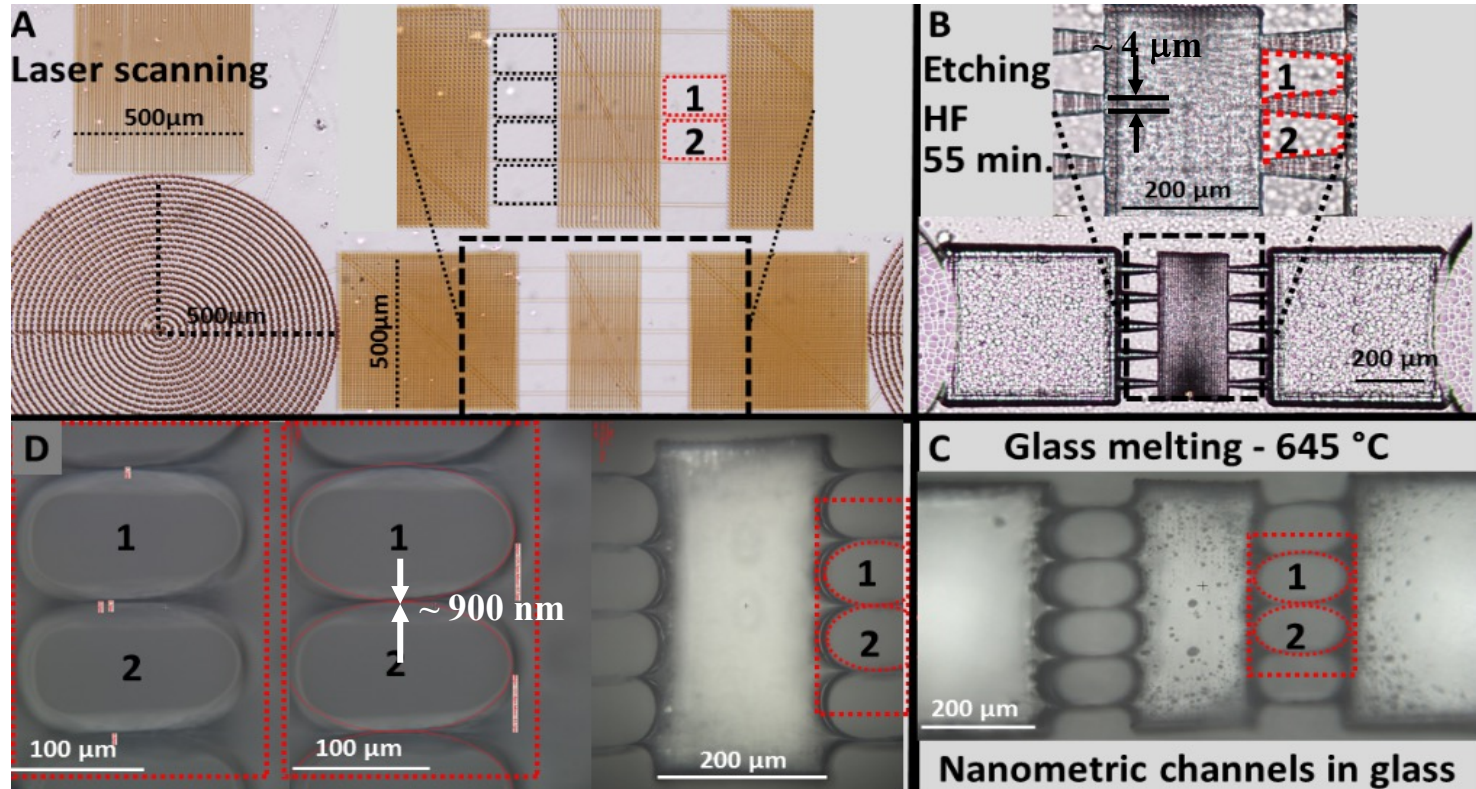
C. M. Denais et al., *Science*, 352, 353 (2016).

Cancer cells can migrate through a constriction with a size of $2 \times 5 \mu\text{m}^2$ using a planer 2D biochip. During the migration, the nucleus is deformed which significantly damages the nuclear envelope, while the damaged nuclear envelope can be repaired after the migration.

Size of cancer cells:
several ~ several tens of μm

Application of 3D microfluidic chip

Mechanism study of cancer cell metastasis and invasion

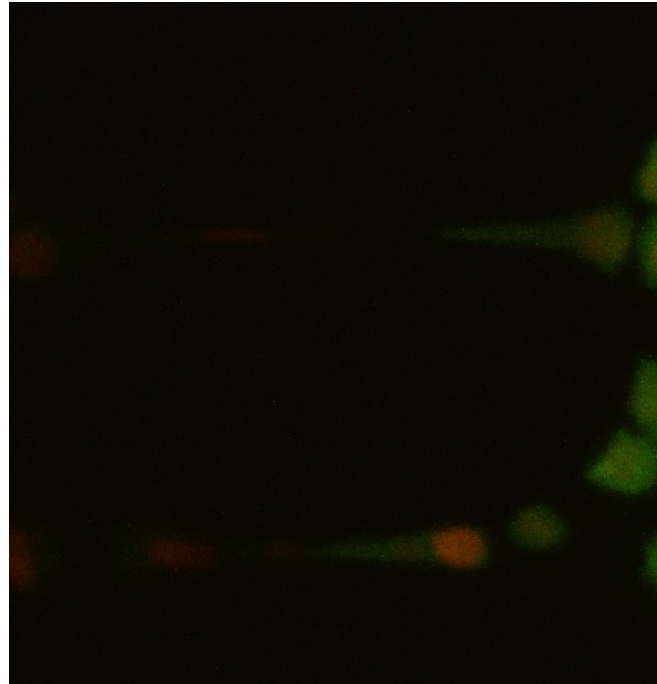


Application of 3D microfluidic chip

Mechanism study of cancer cell metastasis and invasion

Cancer Cells: PC3 (human prostate cancer cell line), No Chemoattractant

*Nuclei are stained with red fluorescent protein,
while the other part, with green fluorescent protein*



**No damage of nucleus envelope
and cell membrane**

Application of 3D microfluidic chip

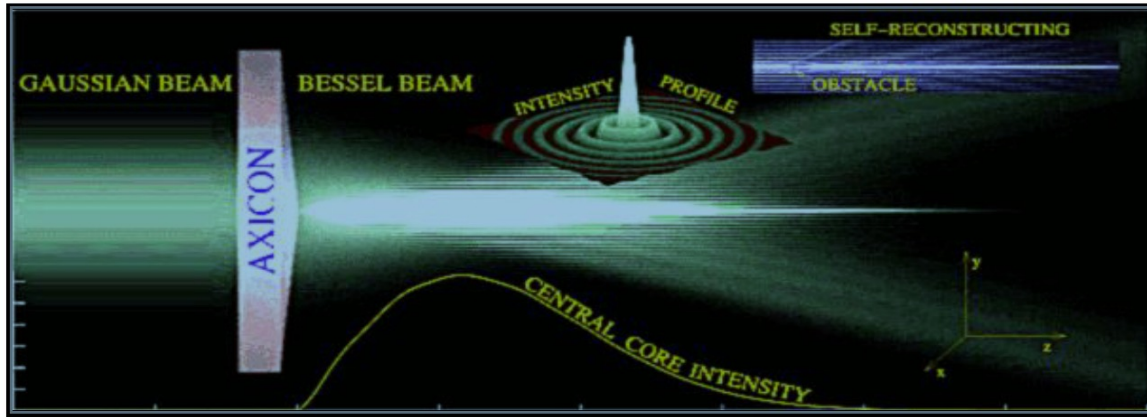
Mechanism study of cancer cell metastasis and invasion

Our findings from observation of cancer cell migrating in the nanochannels.

1. Cells can migrate in nanochannels with a width narrower than $1\ \mu\text{m}$, which is more than one order narrower than the cell size;
2. Cells can migrate in nanochannels even without chemoattractant;
3. Cells are 100% viable and active after migration in nanochannels;
4. Cells can attain speeds up to $1.5\ \mu\text{m}/\text{min}$, which depend on the channel width, i.e., narrower, faster;
5. The volume of cell nucleus is compressed when passing the nanochannels, and the cell nuclei are able to stretch over the length of nanochannel of $50\ \mu\text{m}$ with no damage;
6. The cells are able to divide and proliferate after or even during the migration. The probability of proliferation remains unchanged after the migration;
7. The cells can further migrate through another nanochannel after first migration like intravasation and extravasation;

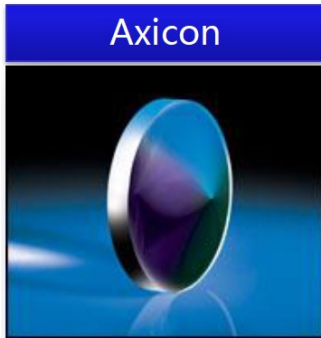
ULAE + Bessel Beam

High-speed, high aspect-ratio glass drilling



Bessel Beam:

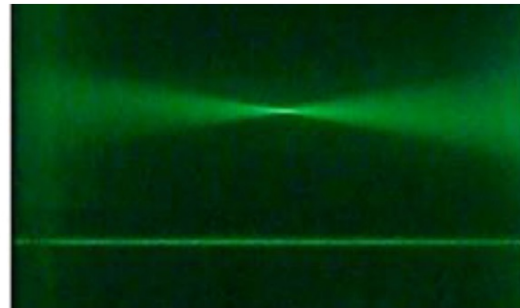
*Amplitude of a Bessel beam is described by a Bessel function of the first kind. A true Bessel beam is non-diffractive. This means that as it propagates, it does not diffract and not spread out; **namely laser beam can remain focused at a long range**, this is in contrast to the usual behavior of light, which spreads out after being focused down to a small spot. The quasi-Bessel beam can be obtained by use of an Axicon lens which has a conical shape.*



Gaussian beam



Bessel beam



SLM is also available for generation of Bessel beam.

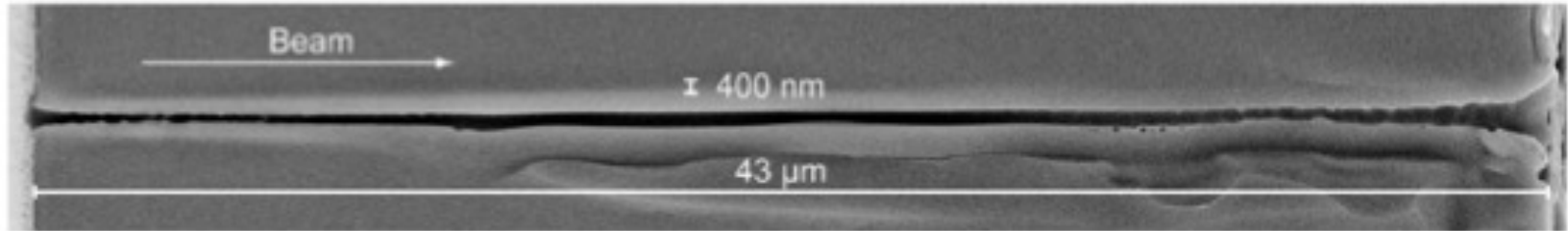
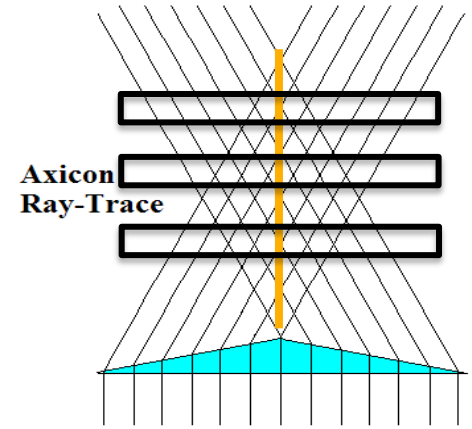
Taper-Free Drilling

Ultrafast laser Bessel beam drilling of glass

- Possibility of high aspect ratio drilling without tapered structures.
- Highly flexible positioning of substrates along the beam axis.

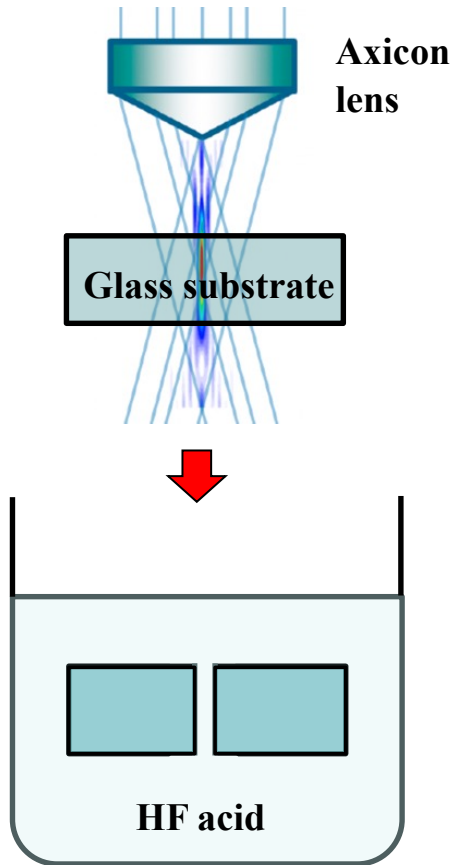


The laser beam must be transparent to the substrate

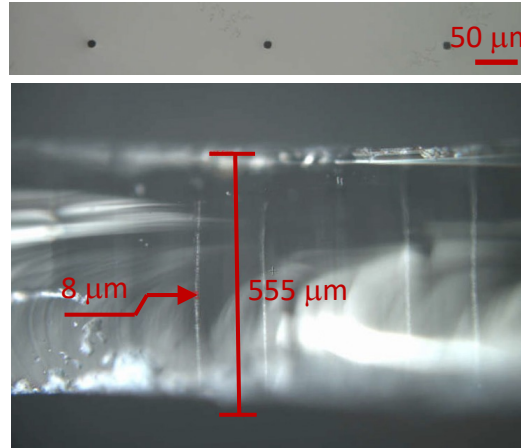


400 nm dia. in 43- μ m thick fused silica glass (aspect ratio: > 100)

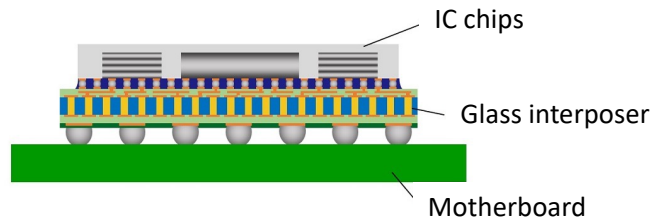
ULAE + Bessel Beam



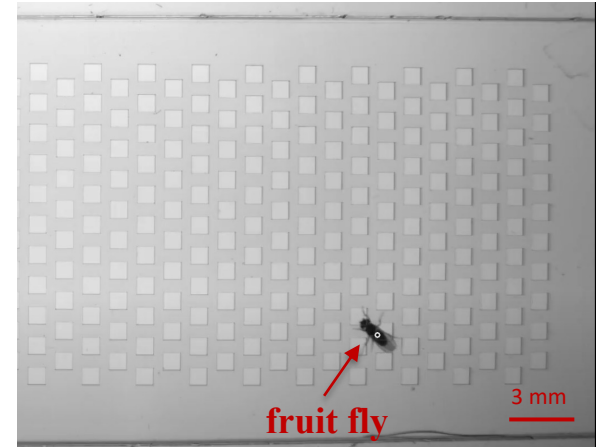
High aspect-ratio through holes for glass interposer for next-generation semiconductor devices



(KOH or NaOH etching)
> 1,000 holes/s



Millimeter size through holes with flexible shape by laser scanning

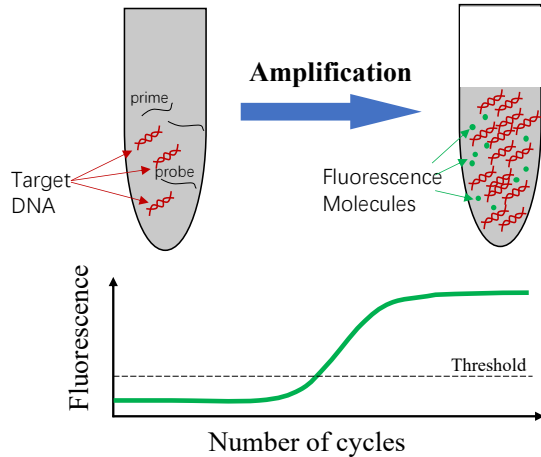


The chip with millimeter size through hole array can be used to study the fast motor control mechanisms that the fruit fly implements for feet placement when it walks over the array of holes.

Digital-PCR

PCR enables drastically amplifying and detecting trace numbers of targeted DNA or RNA molecules in biological samples.

Current PCR Analog Amplification

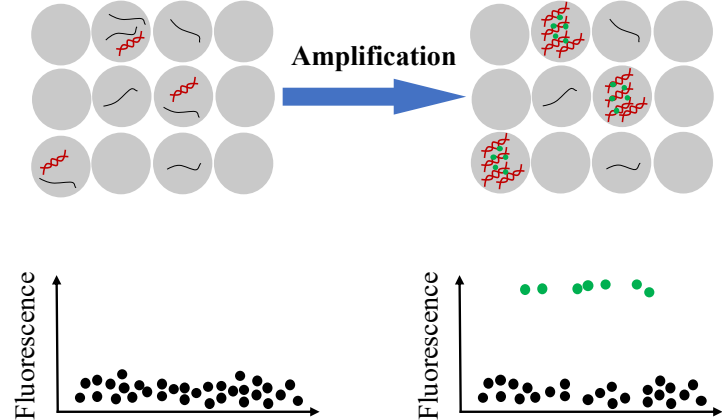


Applications

- ✓ Clinical diagnostics
- ✓ Environmental pathogen monitoring
- ✓ Genetic engineering
- ✓ DNA sequencing

Next-Generation PCR Digital Amplification

Numerous independent units (Unit volume: several nL)

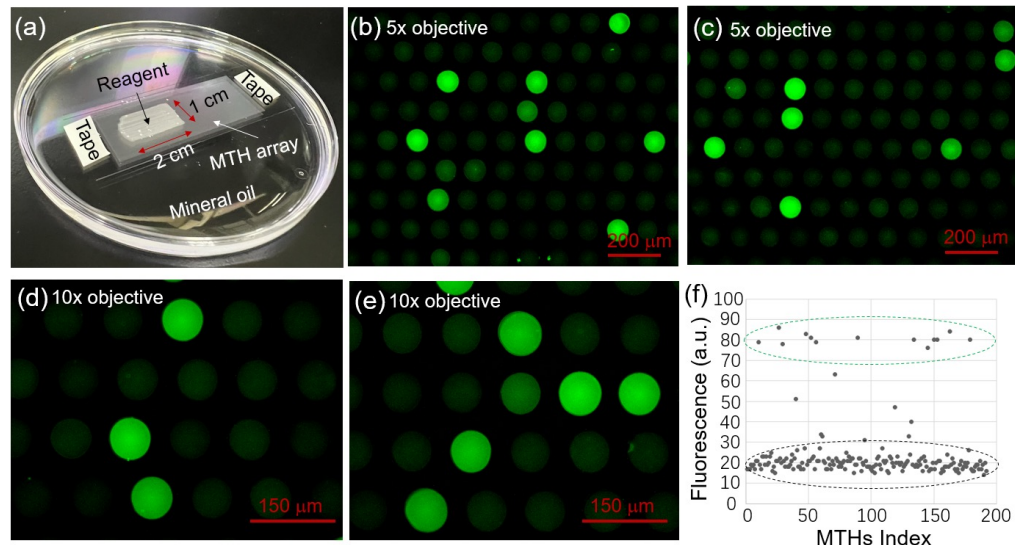
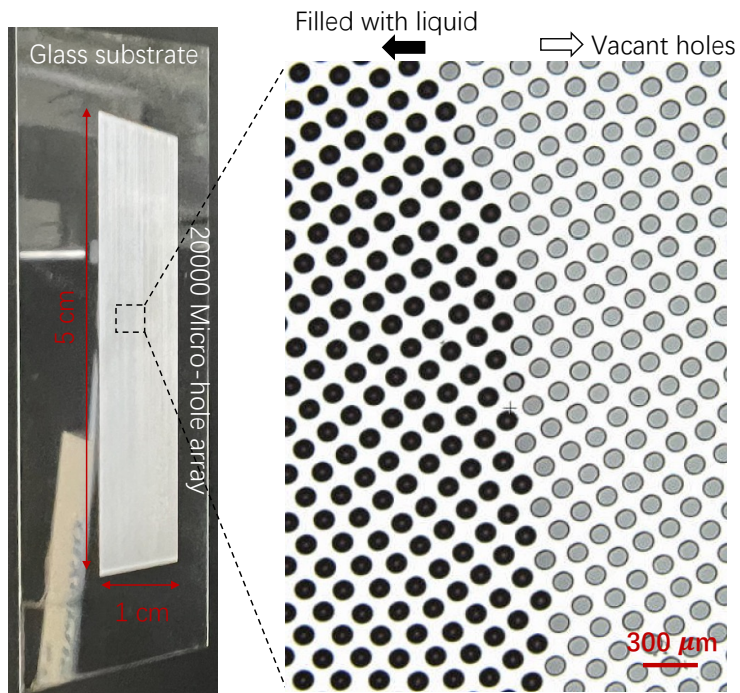


Advantages

- ✓ Increased Sensitivity
- ✓ Absolute Quantification
- ✓ Tolerant to Inhibitors
- ✓ Detection of rare mutations

*Requirement: more than 10,000 microchambers
with a volume of several nL*

Digital PCR Chips Fabricated by Bessel Beam ULAE



20,000 micro-hole array

Substrate: 500 μm thick Borosilicate glass

Etching Selectivity: 4:1 (modified:unmodified)

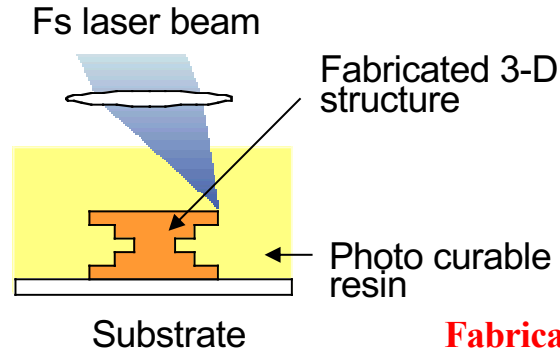
Created holes: ~70 μm diameter, ~400 μm depth

*Array of holes can be created at a speed of 100 holes/s.
(scalable to more than thousands per second).*

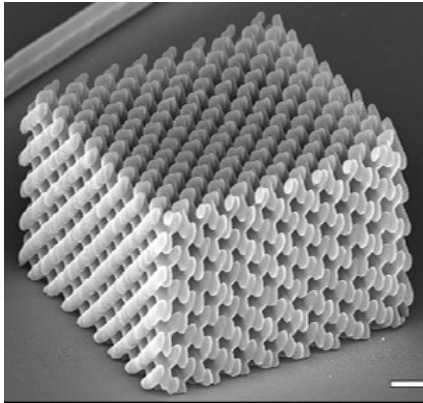
J. Zhang, K. Sugioka et al., Small Sci. 4, 2300166 (2024).

Additive Processing: Two-Photon Polymerization

(Kawata et al., 1997)

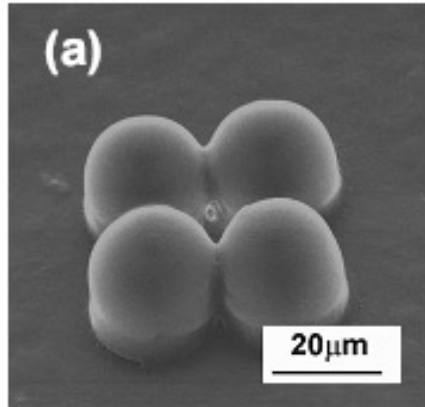


Fabrication resolution: ~100 nm



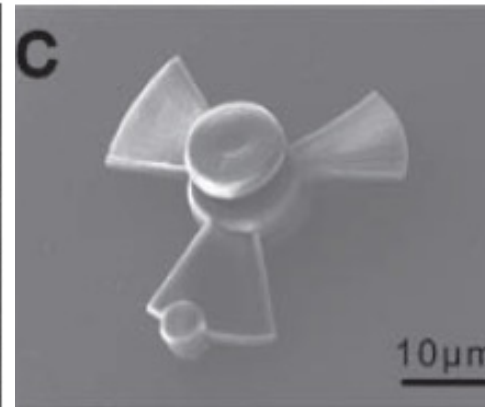
3D photonic crystal

K. K. Seet, et.al, Adv. Mater. **17**, 541 (2005).



3D microlens arrays

R.Guo, et.al, Opt. Express **14**, 810 (2006).

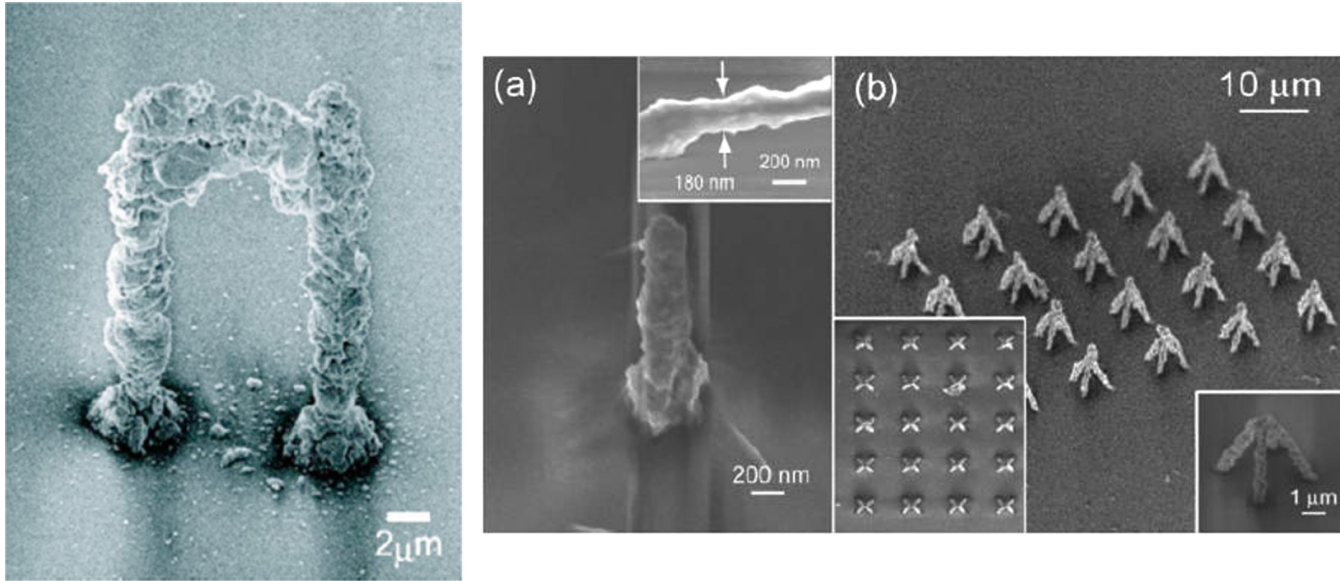


3D microturbine

Adv. Mater. **22**, 3204 (2010).

3D printing of metal micro- and nano-structures

Two-Photon Photoreduction in either a sol-gel matrix, a polymer composite containing metal nanoparticles and a silver salt, a metal-ion solution, or a polymer film containing silver ions



Metal ion solutions

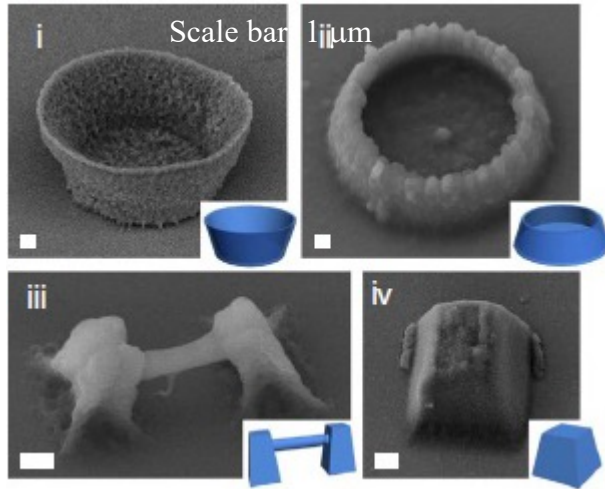
Ag source: diammine silver ions (DSI)

Surfactant: nitrogen atom-containing alkyl carboxylate

(n-decanoylsarcosine sodium; NDSS)

3D printing of protein micro- and nano-structures

Two-photon Crosslinking in mixture of protein molecules and photoinitiator

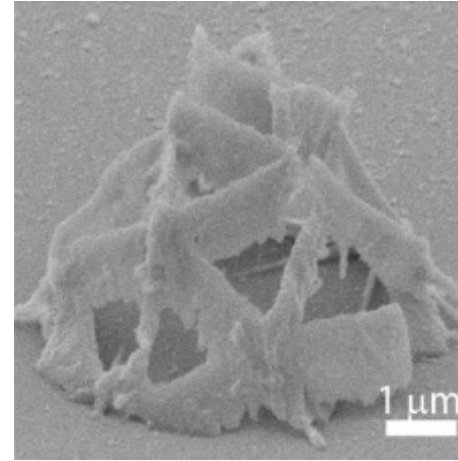


3D printing of all-silk-based micro/nanostructures

Y. L. Sun et al, Nature Commun. **6**, 8612 (2015).

Applications of 3D protein structures:

- Cell culture
- in situ guidance and capture of living cells
- Microactuation due to chemical response (pH dependent volume change)
- Drug delivery



3D printing of pure BSA by photo-initiator free femtosecond laser multiphoton crosslinking

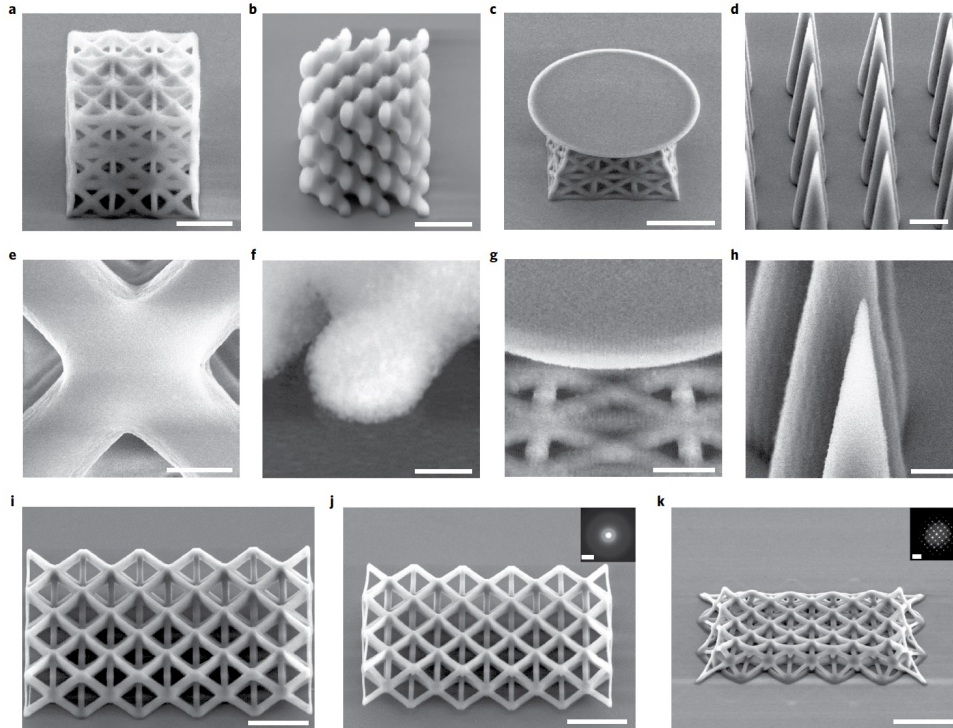
D. Serien and K. Sugioka, ACS Biomater. Sci. Eng. **6**, 1279-1287 (2020).

3D printing of glass micro- and nano-structures

TPP using mixture of photocurable resin and high-density silica nanoparticles

followed by **thermal treatment** at high temperature

T. Doualle et al, Opt. Lett. **46**, 364 (2021).



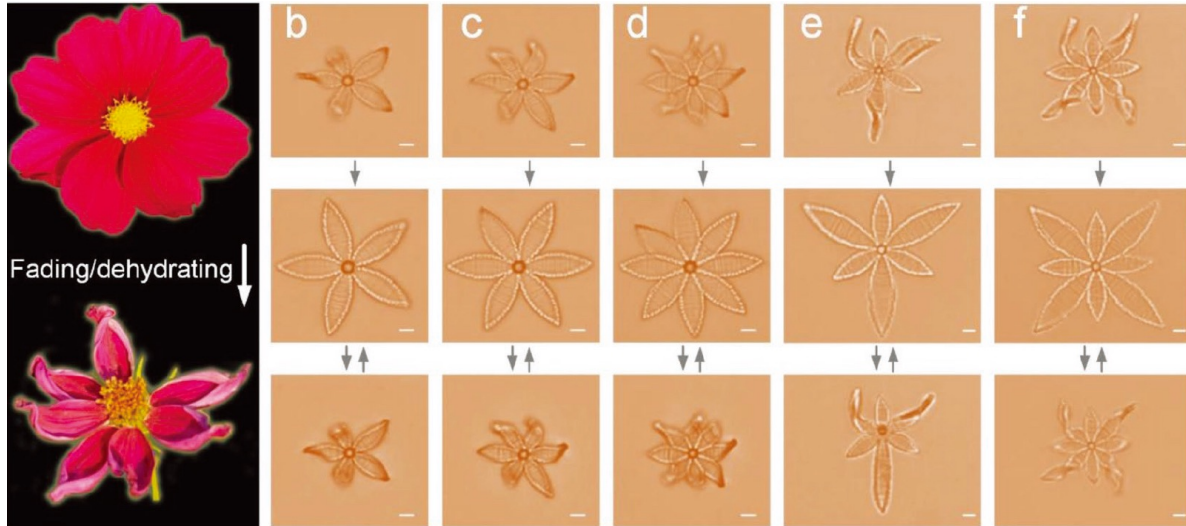
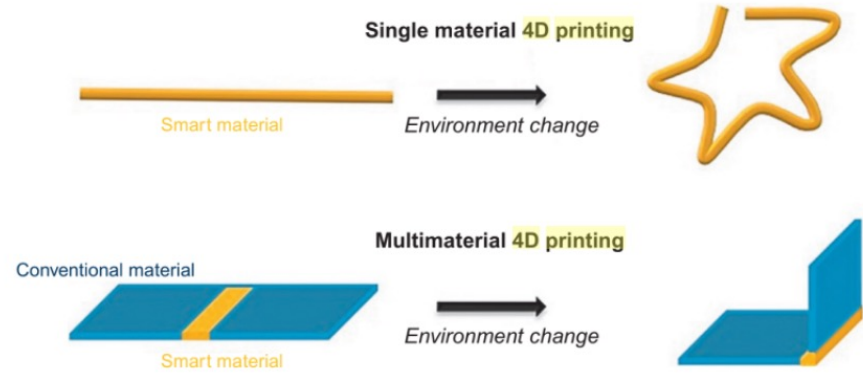
Fabrication resolution: sub-200 nm

Scale bar: (a) 5 μm , (b-d) 10 μm , (e) 400 nm, (f) 1 μm , (g) 2.5 μm , (h) 230 nm, (i-k) 20 μm .

X. Wen et al, Nature Mater. **20**, 1506 (2021).

New Trend: 4D Printing

4D printing introduces the dimension of transformation over time to 3D printed objects. Therefore, after the fabrication process, the printed objects change their forms by changing the environment such as humidity, temperature, pH or applying stimulus with light, magnetic field, etc.



Botanical-Inspired Complex Shape Transformation

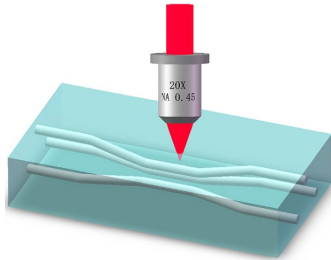
- *4D printing of pH-responsive hydrogel.*
- *Response speed faster than 400 ms.*

Y. Fu et al., Adv. Funct. Mater. **30**, 1907377 (2020)

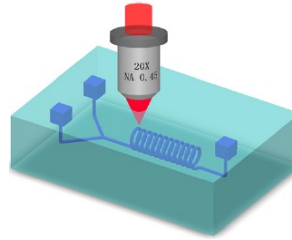
3. Hybrid Ultrafast 3D Processing

Ultrafast Laser 3D Processing

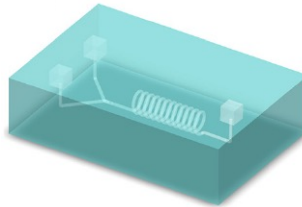
Undeformative processing (Zero processing)



Subtractive processing

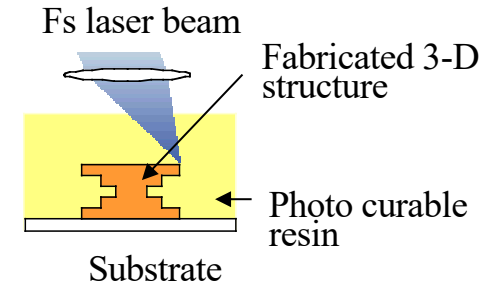


(1) Fs laser direct writing



(2) HF etching

Additive processing



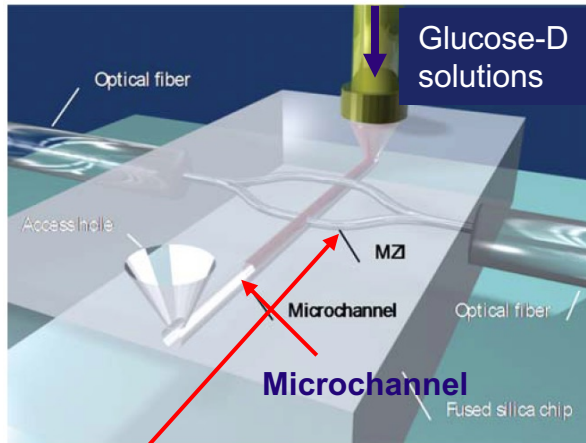
Each scheme has both strong and weak points for 3D fabrication. One scheme can create NOT any kinds of 3D structures.

Hybrid 3D processing will further enhance performance of ultrafast laser 3D microprocessing, and thereby enhance functionality of micro- and nano-devices.

Hybrid Subtractive and Undeformative Processing

ULAE + optical waveguide: Optofluidics for highly sensitive sensor

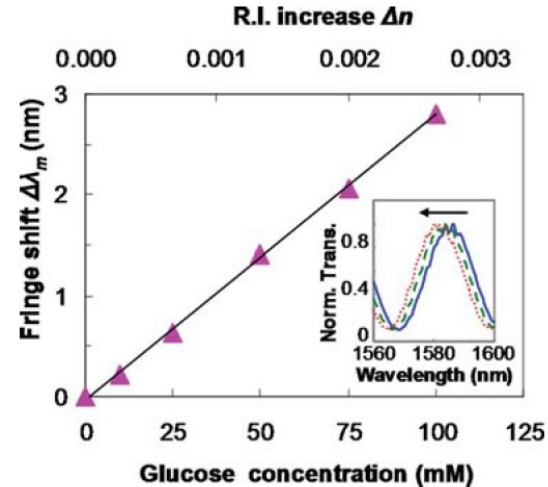
Mach-Zehnder unbalanced interferometer integrated with microchannel can detect reflective index change with a sensitivity of 1×10^{-4} and thereby can clearly distinguish glucose with a concentration of 4 mM.



Mach-Zehnder unbalanced interferometer based on branching optical waveguides, one of which is across the microchannel.

$$\Delta\lambda_m = -\frac{L}{\lambda_m} \Lambda \cdot \Delta n$$

A. Crespi et al., Lab on a Chip, **10**, 1167 (2010).



$$\Lambda = \frac{\lambda_0}{n_0 \Delta s + L \Delta n}$$

$\Delta\lambda_m$: wavelength shift

Δn : refractive index change

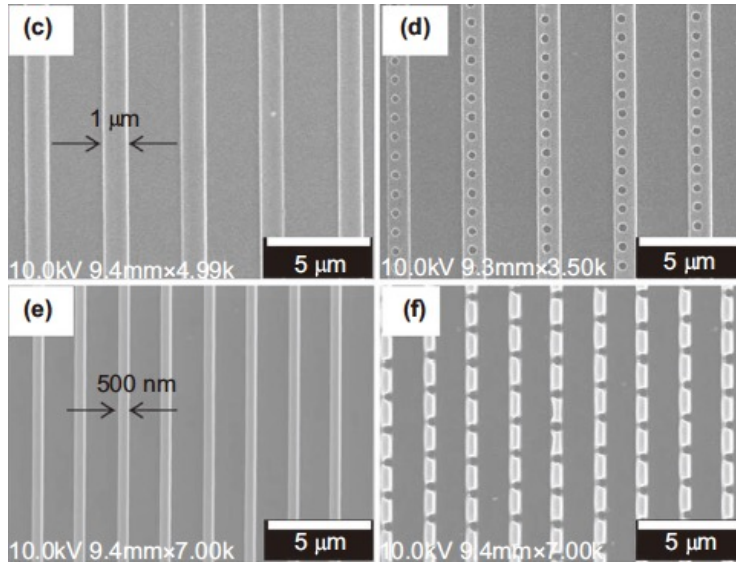
L: length of interferometer

Λ : length difference of two arms

Hybrid Additive and Subtractive Processing

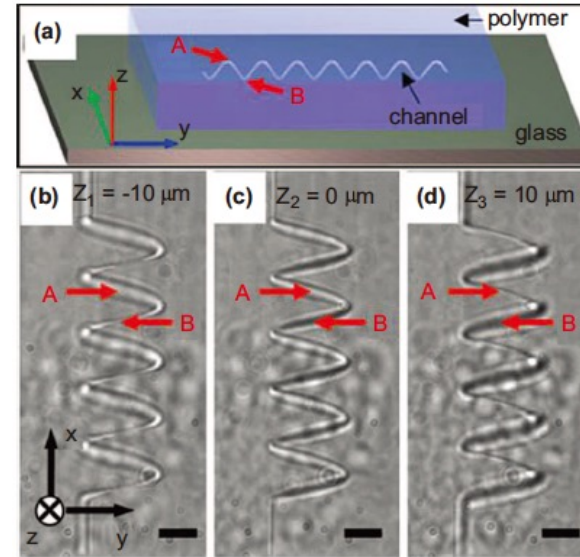
TPP + nano ablation

diversify 3D nanostructures with complicated shapes that cannot be achieved by a single scheme of 3D processing



TPP

TPP+FLA

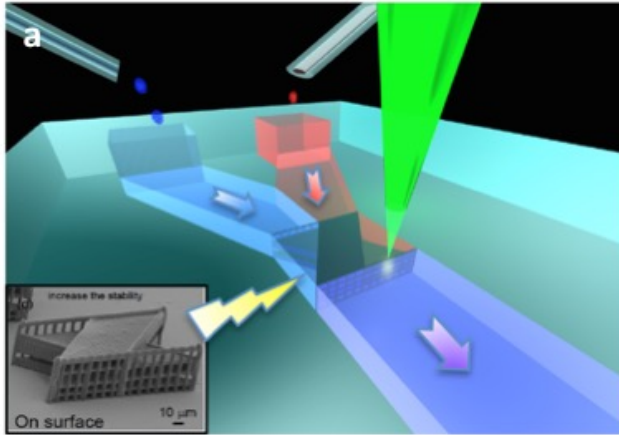
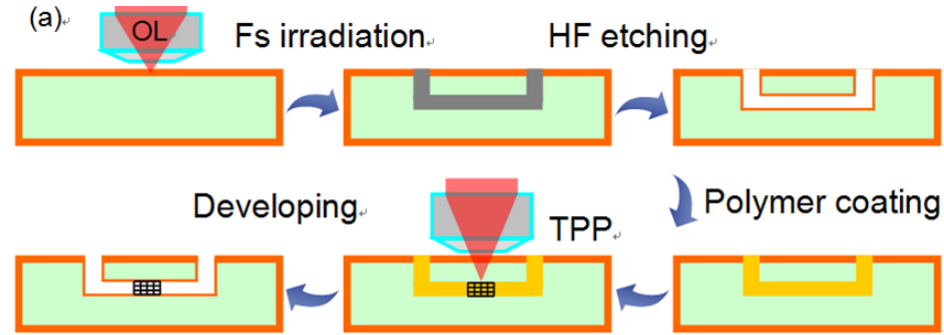


Spiral microfluidic channel
inside polymer

Hybrid subtractive and additive 3D processing ULAE + TPP



*Ship-in-a-bottle
integration*



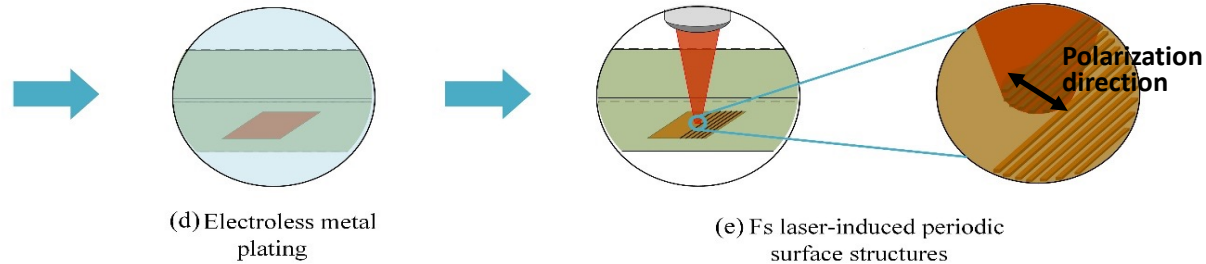
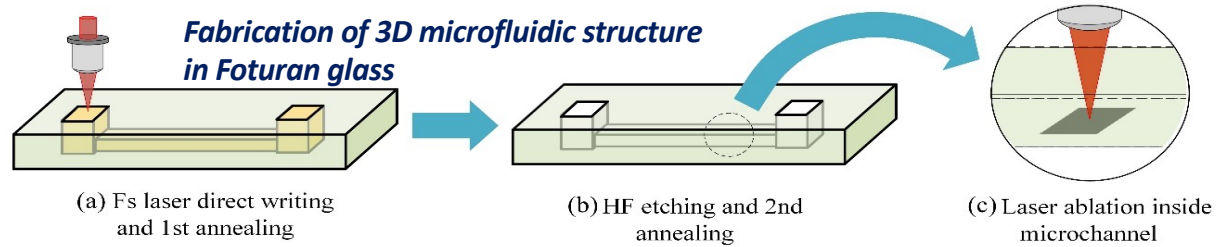
**Integration of mixer
in 3D microfluidics**



D. Wu, K. Sugioka et al., *Laser Photon. Rev.* **8**, 458 (2014).
D. Wu, K. Sugioka et al., *Light Sci. Appl.* **4**, e228 (2015).

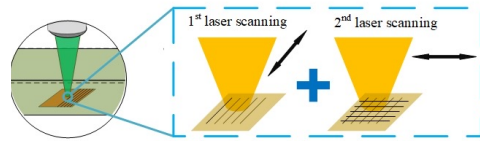
Hybrid subtractive, additive and subtractive processing

Fabrication of 3D microfluidic SERS chips



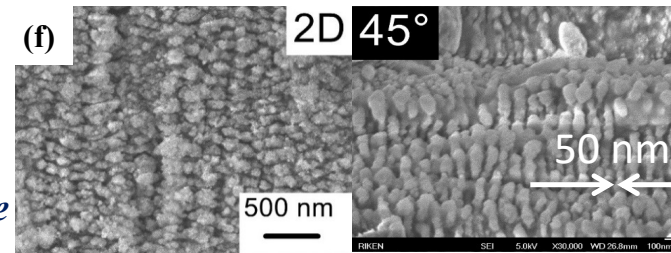
Selective deposition of metal thin film inside microfluidic channel

Nanostructuring of metal thin film with LIPSS



Double-exposure of fs laser beam with orthogonal polarization directions

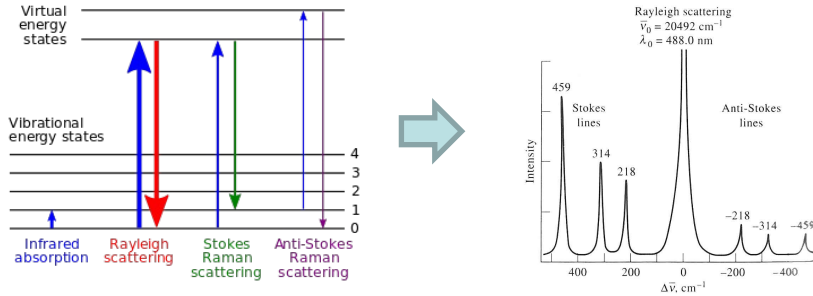
Formation of 2D array of metal nanodot structure



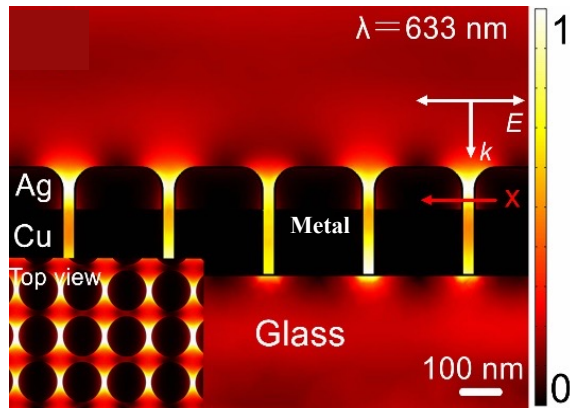
Hybrid subtractive, additive and subtractive processing

SERS (surface enhanced Raman scattering)

Raman spectroscopy



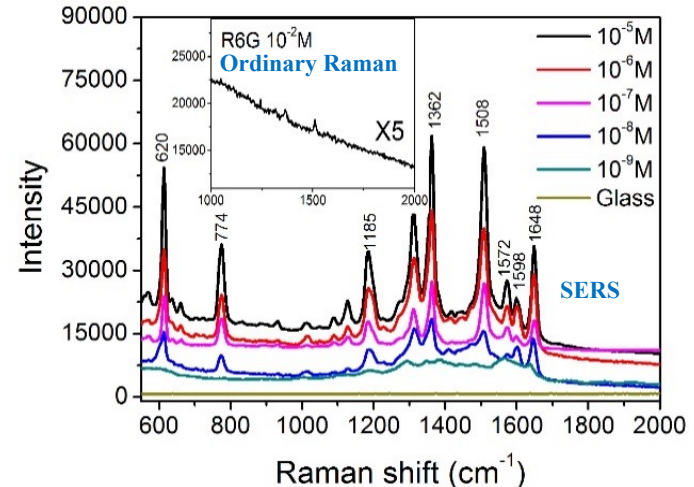
SERS



Electric field is strongly enhanced in the vicinity of metal nanostructures by localized surface plasmon resonance (LSPR)

Raman spectroscopy is a spectroscopic technique typically used to determine vibrational modes of molecules, which enables us to identify molecules and study chemical bonding and intramolecular bonds. Thus, Raman spectroscopy is widely used as one of the most common materials characterization methods in science and engineering, including identification of substances and quantitative analysis of concentrations.

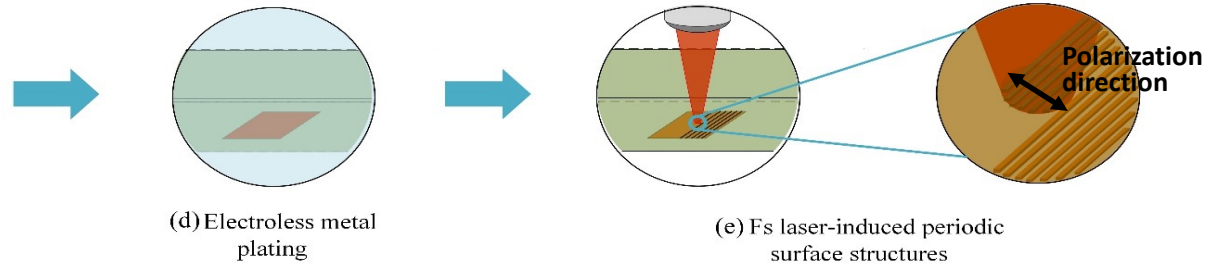
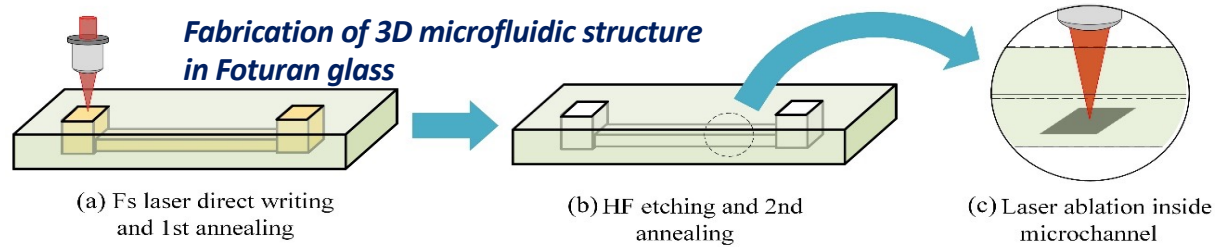
Drawback: Low sensitivity



Raman signals can be enhanced by a factor of $10^5 \sim 10^8$ for highly-sensitive analysis of materials

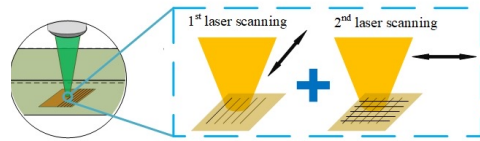
Hybrid subtractive, additive and subtractive processing

Fabrication of 3D microfluidic SERS chips



Selective deposition of metal thin film inside microfluidic channel

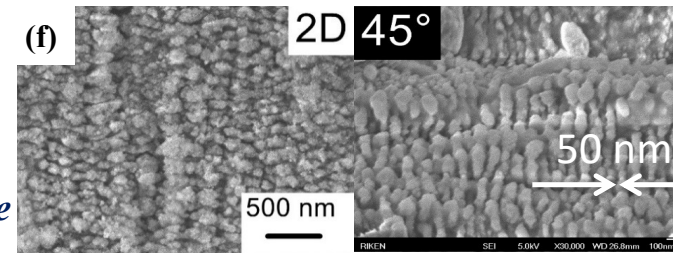
Nanostructuring of metal thin film with LIPSS



(5) Fs laser-induced 2D periodic surface structures

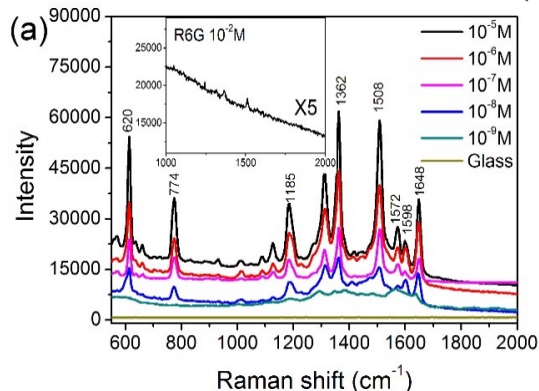
Double-exposure of fs laser beam with orthogonal polarization directions

Formation of 2D array of metal nanodot structure



Hybrid subtractive, additive and subtractive processing Characterization of 3D Microfluidic SERS Chips

Analytical enhancement factor (AEF)



$$AEF = (I_{SERS}/I_{OR}) / (C_{SERS}/C_{OR})$$

I_{SERS} : Raman intensities on the SERS substrate

I_{OR} : Raman on glass

C_{SERS} : molar concentration on the SERS substrate (10⁻⁹ M)

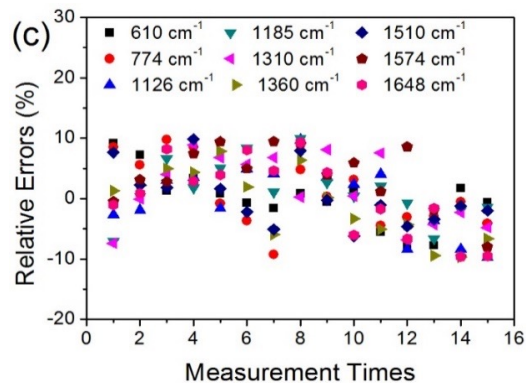
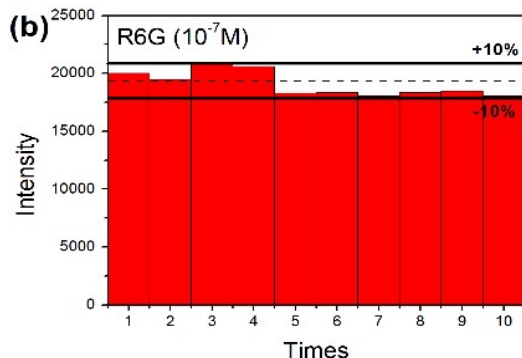
C_{OR} : molar concentration glass (10⁻¹ M)

Test sample : Rhodamine 6G

AEF $\sim 7.3 \times 10^8$ (cf. typical EF: 10⁵ ~ 10⁸)

Detection limit ~ 1 nM

Relative standard deviation (RSD)

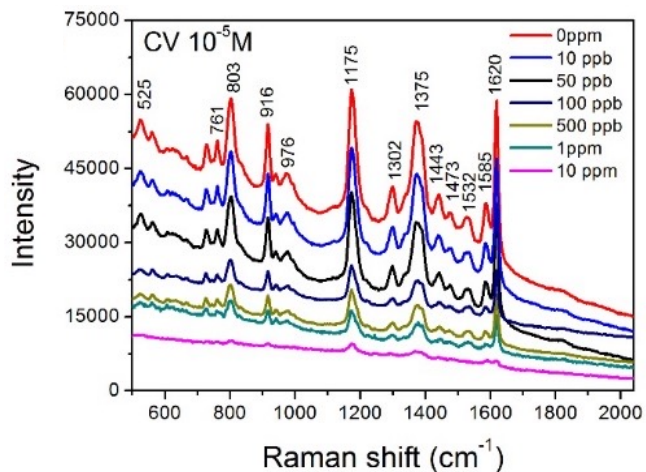
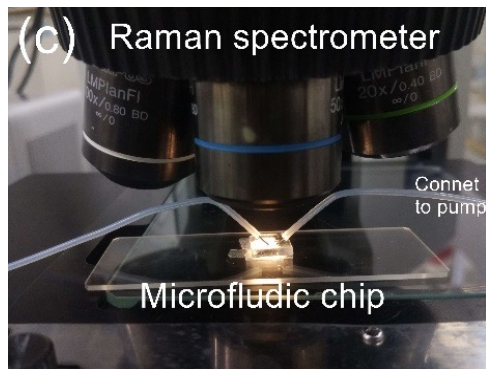


RSD $\sim 8.8\%$

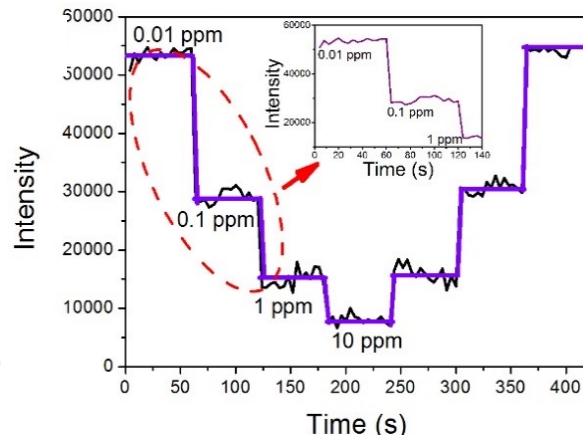
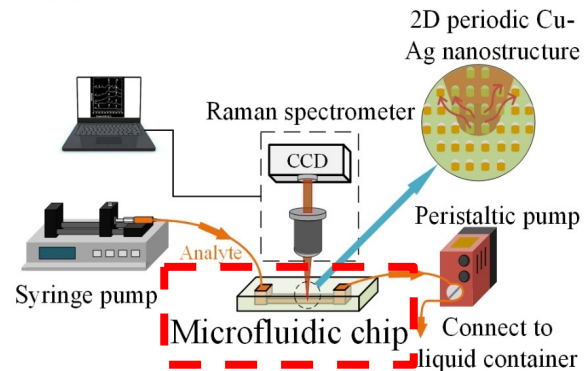
(< 10%, sufficiently small for practical use)

Hybrid subtractive, additive and subtractive processing

Real-time SERS sensing of Cd^{2+} ions



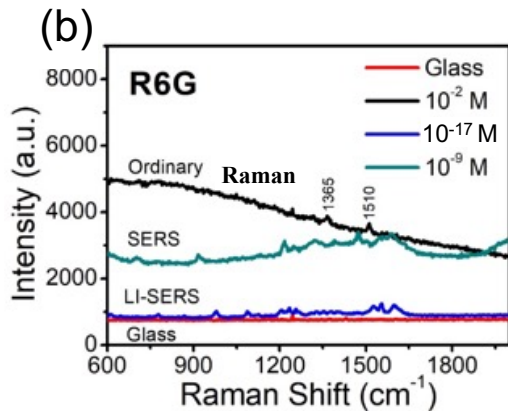
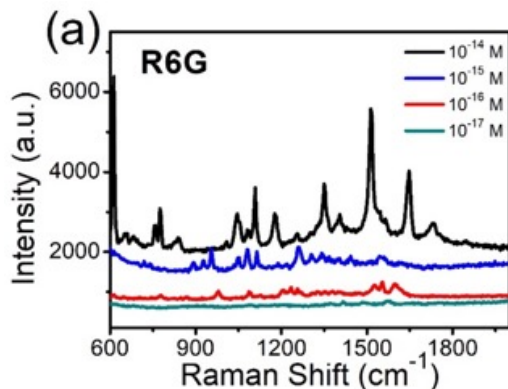
Detection limit: 10 ppb



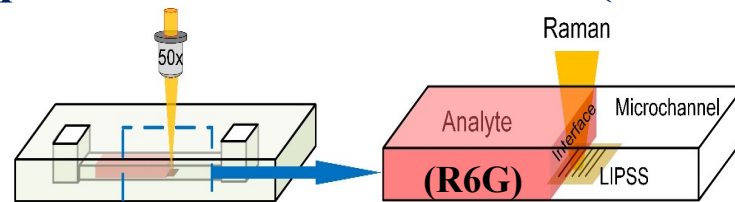
Real-time sensing of Cd^{2+} solutions with different concentration over time

Hybrid subtractive, additive and subtractive processing

Attomolar sensing



Liquid-Interface assisted SERS (LI-SERS)



$AEF_{LI-SERS} = 1.52 \times 10^{14}$
(cf., $AEF_{O-SERS} = 7.3 \times 10^8$)
Detection limit (R6G) < 10 aM



1 eye drop

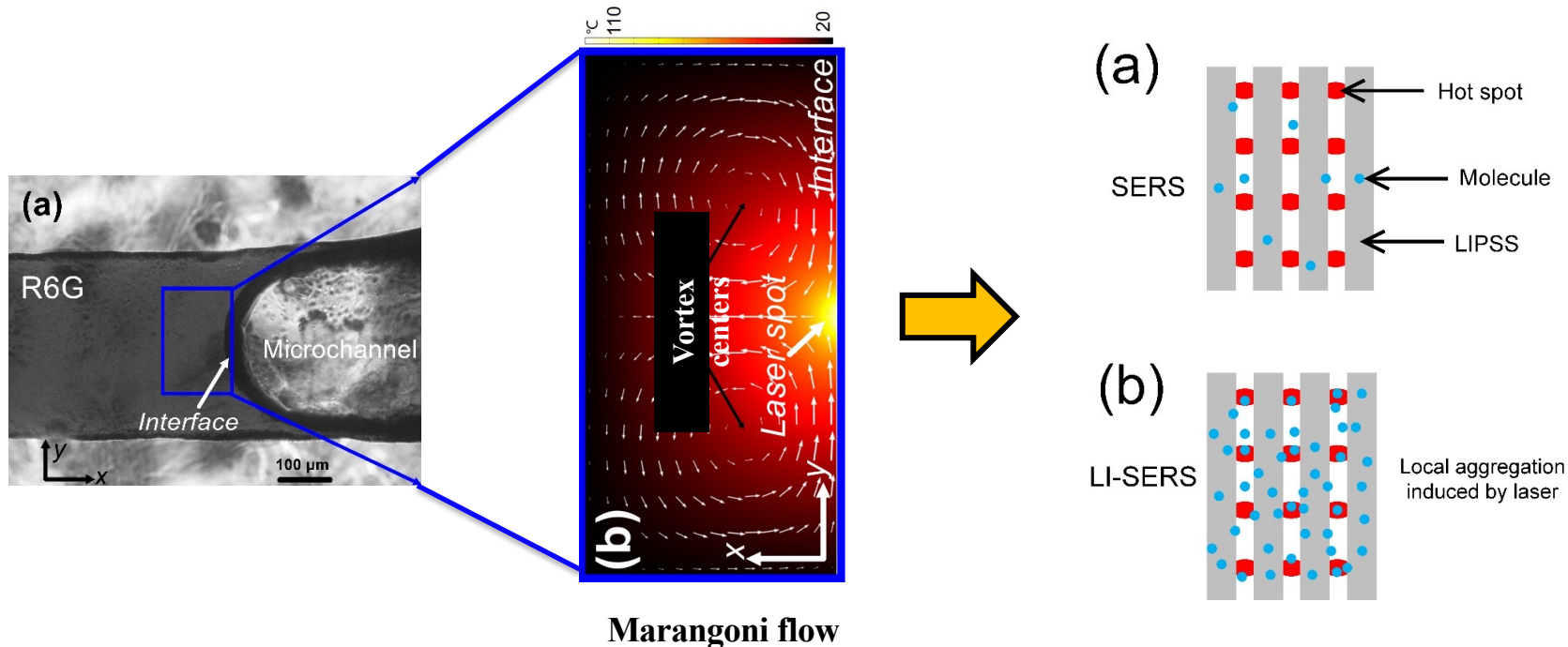


2 x New National Stadium Japan

for Tokyo 2020/2021 Olympic and Paralympic Games

Hybrid subtractive, additive and subtractive processing

Mechanism of LI-SERS



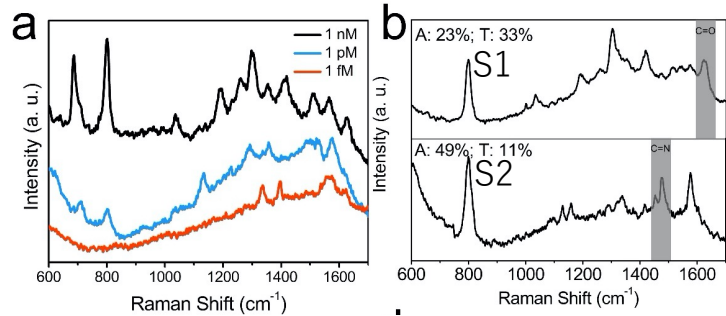
(1) Generation of Marangoni flow by laser heating to collect analyte molecules to the laser spot

(2) Optical trapping of collected analyte molecules by enhanced electric fields at hot spots

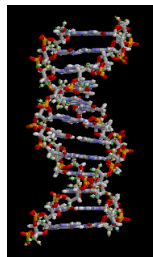
Sensing of Biomolecules with Large Molecular Weights

Liquid-Interface Assisted SERS (LI-SERS)

DNA discrimination

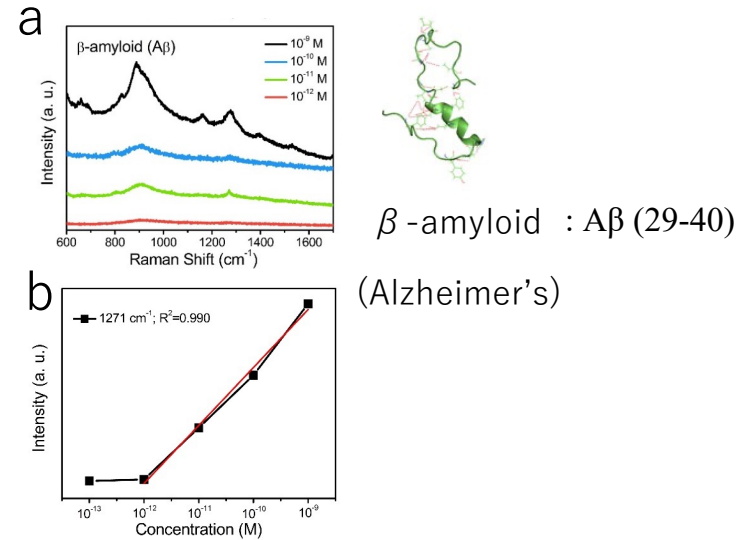


Concentration (DNA sequence) 1 fM



Sequence (10 fM)	A	T	C	G
S1: TCCACAACCATGTCCTGATAGTTTTTCAGC	23.33%	33.33%	30%	13.33%
S2: TAAATACAAGTACCATCAGGCGAAACACAAACAGC	48.57%	11.43%	25.71%	14.29%

Diagnosis of disease in early-stage



Detection limit < 1 pM (Label-free)

4. Summary

- **The efficient confinement of nonlinear interactions within sub-diffraction focal volumes has led to the realization of ultrafast laser 3D micro and nanofabrication with 100 nm resolution for additive TPP, in addition to undeformative writing of optical waveguides and the subtractive fabrication of microfluidic channels in bulk transparent materials by internal processing.**
- **The flexibility of the direct writing scheme that employs scanning of tightly focused ultrafast laser pulses has enabled the formation of various 3D micro/nanostructures with almost unlimited geometries and configurations, which has had a significant impact on a broad range of applications ranging from optoelectronics, photonics and MEMS to chemical, biological and medical systems.**
- **A new strategy, in which synergetic combination of each 3D processing into a hybrid approach, has opened up a new door to enhance the flexibility and/or capability of 3D ultrafast laser micro and nanofabrication by taking advantages of complementary characteristics of each individual approach.**

Ultrafast lasers—reliable tools for advanced materials processing

Koji Sugioka¹ and Ya Cheng²

The unique characteristics of ultrafast lasers, such as picosecond and femtosecond lasers, have opened up new avenues in materials processing that employ ultrashort pulse widths and extremely high peak intensities. Thus, ultrafast lasers are currently used widely for both fundamental research and practical applications. This review describes the characteristics of ultrafast laser processing and the recent advancements and applications of both surface and volume processing. Surface processing includes micromachining, micro- and nanostructuring, and nanoablation, while volume processing includes two-photon polymerization and three-dimensional (3D) processing within transparent materials. Commercial and industrial applications of ultrafast laser processing are also introduced, and a summary of the technology with future outlooks are also given.

Light: Science & Applications (2014) 3, e149; doi:10.1038/lisa.2014.30; published online 11 April 2014

Keywords: 3D fabrication; industrial application; micromachining; nanofabrication; ultrafast laser

INTRODUCTION

Materials processing using ultrafast lasers, lasers that emit light pulses shorter than a few tens of picoseconds, was first reported in 1987 by Srinivasan *et al.*¹, Küper and Stuke.² They demonstrated the clean ablation of polymethyl methacrylate almost without the formation of a heat-affected zone (HAZ) using femtosecond ultraviolet excimer lasers. The ablation threshold was

glass and polymers.^{11–14} Davis *et al.*¹¹ and Glezer *et al.*¹² pioneered this field and demonstrated respectively optical waveguide writing and formation of nanovoid arrays inside glass in 1996. Currently, internal microfabrication is widely applied to the fabrication of photonic devices and biochips.^{15,16} It was also reported in 2001 that multiphoton absorption improves spatial resolution to exceed the diffraction limit, due to the nonlinearity combined with the

Femtosecond laser three-dimensional micro- and nanofabrication

Koji Sugioka^{1,a)} and Ya Cheng^{2,b)}

¹*RIKEN Center for Advanced Photonics, Hirosawa 2-1, Wako, Saitama 351-0198, Japan*

²*Shanghai Institute of Optics and Fine Mechanics, Chinese Academy of Sciences, P.O. Box 800-211, Shanghai 201800, China*

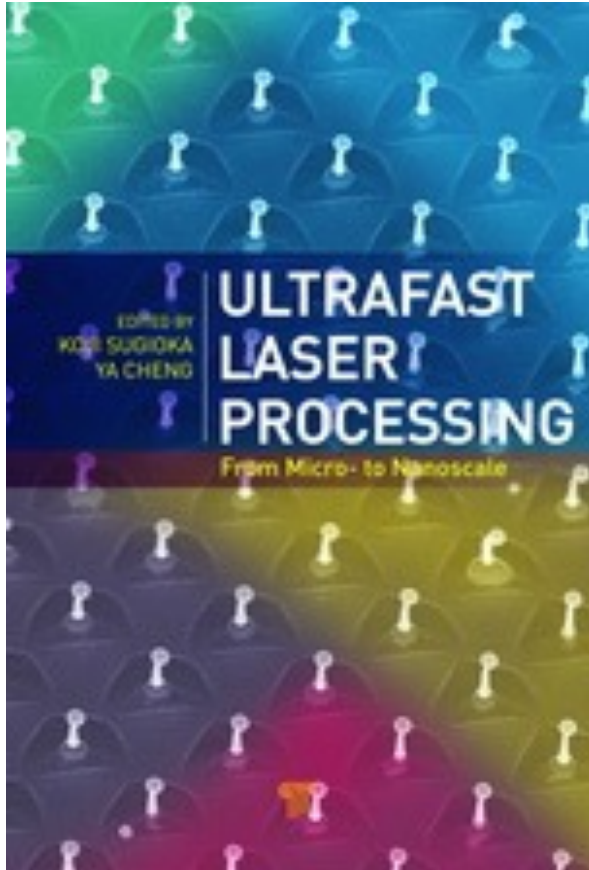
(Received 17 October 2014; accepted 25 November 2014; published online 23 December 2014)

The rapid development of the femtosecond laser has revolutionized materials processing due to its unique characteristics of ultrashort pulse width and extremely high peak intensity. The short pulse width suppresses the formation of a heat-affected zone, which is vital for ultrahigh precision fabrication, whereas the high peak intensity allows nonlinear interactions such as multiphoton absorption and tunneling ionization to be induced in transparent materials, which provides versatility in terms of the materials that can be processed. More interestingly, irradiation with tightly focused femtosecond laser pulses inside transparent materials makes three-dimensional (3D) micro- and nanofabrication available due to efficient confinement of the nonlinear interactions within the focal volume. Additive manufacturing (stereolithography) based on multiphoton absorption (two-photon polymerization) enables the fabrication of 3D polymer micro- and nanostructures for photonic devices, micro- and nanomachines, and microfluidic devices, and has applications for biomedical and tissue engineering. Subtractive manufacturing based on internal modification and fabrication can realize the direct fabrication of 3D microfluidics, micromechanics, microelectronics, and photonic microcomponents in glass. These microcomponents can be easily integrated in a single glass microchip by a simple procedure using a femtosecond laser to realize more functional microdevices, such as optofluidics and integrated photonic microdevices. The highly localized multiphoton absorption of a tightly focused femtosecond laser in glass can also induce strong absorption only at the interface of two closely stacked glass substrates. Consequently,

Koji Sugioka
Editor

Handbook of Laser Micro- and Nano- Engineering

This handbook provides a comprehensive review of the entire field of laser micro and nano processing, including not only a detailed introduction to individual laser processing techniques but also the fundamentals of laser-matter interaction and lasers, optics, equipment, diagnostics, as well as monitoring and measurement techniques for laser processing. It consists of 3 volumes including 11 sections, each composed of 4 to 6 chapters for a total of 57 chapters (2099 pages in total), written by leading experts in the relevant field.



Ultrafast Laser Processing - From Micro- to Nanoscale

*by Koji Sugioka (RIKEN, Japan),
Ya Cheng*

Pan Stanford Publishing, Inc.

Hardback

12 chapters, 616 pages

2013-06-30

Print ISBN: 9789814267335

eBook ISBN: 9789814303699

DOI: 10.4032/9789814303699

List price : **\$149.95**